2018-11

Friction stir welds in aluminium: Design S-N curves from statistical analysis of literature data

Maggiolini, E

10.1111/ffe.12805
Fatigue and Fracture of Engineering Materials and Structures
Wiley

Friction stir welds in aluminium: design S-N curves from statistical analysis of literature data

E. Maggiolini[1], D. Benasciutti[1 *], L. Susmel[2], D.G. Hattingh[3], M.N. James [3, 4], R. Tovo[1]

[1] Department of Engineering, University of Ferrara, via Saragat 1, 44122 Ferrara (Italy)

[2] Department of Civil and Structural Engineering, University of Sheffield, Sheffield S1 3JD, United Kingdom

[3] Department of Mechanical Engineering, Nelson Mandela University, Port Elizabeth 6000, South Africa

[4] School of Engineering, University of Plymouth, Drake Circus, Devon PL4 8AA, Plymouth, United Kingdom

Abstract

Appropriate S-N fatigue design curves for friction stir (FS) welded joints in aluminium alloys are currently not specified in design codes and standards. The present paper is intended to assist in enabling standardised fatigue design for such joints, through a comprehensive statistical analysis of more than 500 individual sets of data gathered from published literature. These data are used to establish the usual design fatigue curves for welds that give a 97.7% survival probability with 95% confidence. Experimental fatigue data represent defect-free butt joints and include both flat plate and tubular joints between similar aluminium alloys (across the range of 2xxx, 5xxx, 6xxx, and 7xxx series). Weld conditions include as-welded, machined, and post-weld heat treated under constant amplitude cyclic loading at various stress ratios in the range from R = -1 to 0.5. A systematic comparison is presented by categorising the data according to the alloy type, temper condition, post-weld heat treatment and stress ratio and the correlation with the S-N design curves from Eurocode 9 is also considered. The fatigue curves presented in this paper will serve as a useful guideline for engineers involved in design of friction stir aluminium joints subjected to in-service fatigue loading.

Keywords:

Friction stir (FS) welding; aluminium alloy; fatigue loading; design S-N curve; statistical analysis.

---

* Corresponding author:
Denis Benasciutti, e-mail: denis.benasciutti@unife.it
Phone: +39 (0)532 974976 Fax: +39 (0)532 974870

Nomenclature

a, b	intercept and slope of the regression line
k	inverse slope of S-N line
n	number of specimens tested at a specific stress range (sample size)
N	number of cycles to failure
N_A	reference number of cycles to failure ($N_A=2\times10^6$)
$N_{97.7\%}$	estimated number of cycles to failure, for $P_s=97.7\%$
$N_{97.7\%,95\%}$	estimated number of cycles to failure, for $P_s=97.7\%$ and $\gamma=95\%$
$N_{2.3\%,95\%}$	estimated number of cycles to failure, for $P_s=2.3\%$ and $\gamma=95\%$
P_s	survival probability
s^2	sample variance
$t_{(\gamma;n-2)}$	one-tail γ-percentile of Student's t-distribution with $(n-2)$ degrees of freedom
$x=\log(\Delta\sigma)$	transformed stress range
$y=\log(N)$	transformed number of cycles to failure
γ	confidence
ε	zero-mean normally distributed random variable
$\Delta\sigma$	stress range
$\Delta\sigma_{A,50\%}$	fatigue strength at N_A cycles to failure, for $P_s=50\%$
$\Delta\tilde{\sigma}_{A,97.7\%}$	fatigue strength at N_A cycles to failure, for $P_s=97.7\%$ (without confidence)
$\Delta\sigma_{A,97.7\%}$	fatigue strength at N_A cycles to failure, for $P_s=97.7\%$ and $\gamma=95\%$
$\Delta\sigma_{A,2.3\%}$	fatigue strength at N_A cycles to failure, for $P_s=2.3\%$ and $\gamma=95\%$
$\Phi(-)$	standard normal cumulative distribution function
AA	artificially aged
NA	naturally aged
PWAT	post-weld ageing treatment
PWHT	post-weld heat treatment

Introduction

Since its launch at TWI in 1991, several specific features of friction stir (FS) welding have led to a substantial industrial impact as a joining technique across many engineering areas that include ground transportation, ships, aircrafts, and the nuclear and space industries[1,2]. It is a solid-state autogenous process that provides joints with a fine-grained nugget that are generally free from gross porosity and solidification cracks, and have relatively low thermal distortion and residual stresses[1]. Thanks to these distinctive features, FS welded joints are often characterised by mechanical properties (particularly fatigue strength) that are superior to those pertaining to conventional fusion arc welds. Even in the presence of several defect types that are unique to FS welding of certain aluminium alloys (e.g. [3]) fatigue strengths for as-welded joints in the range 70 MPa to 100 MPa can be obtained in reversed bending (R = -1) at lives of 2 x 10^6 cycles.

The increasing interest in the technology, metallurgy and mechanical properties of FS welding is clearly demonstrated by the exponential growth in published papers over the last twenty years[1]. Considerable attention has been devoted to characterising the fatigue strength of FS joints subjected to cyclic loading, and to exploring influential factors (e.g. type of parent material, welding process parameters, residual stresses, surface finishing, and stress ratio) and identifying optimum process conditions and tool geometries (e.g. [4]). Several studies have confirmed that the fatigue resistance of FS welds in aluminium alloys is generally superior to fusion welds, regardless of parent material, welding process and loading condition. For example, [5,6,7] have observed that FS welded joints in aluminium have a fatigue strength higher than arc-welded joints, potentially with an increment of three times that seen in MIG[8] and TIG[9] welds in 6xxx aluminium alloy. Reference [10] demonstrates that FS welded aluminium joints have a fatigue resistance above the design line in the Eurocode 9 standard for butt-welds made from one side[11].

Although a large amount of fatigue data on FS welds, published by various authors, is now available, a codified standard or formal set of guidelines to assist engineers in designing FS welds against fatigue does not yet exist (in contrast to the situation for fusion welds, which are supported by, for example, European Standards[12,13] and IIW recommendations[14]). In 2005, Lomolino et al.[15] made a first attempt to derive reference fatigue curves for several types of FS aluminium welds, based on a statistical analysis of hundreds of data. Their results suggested that fatigue data should be categorised according to several influential factors (parent material, temper condition, welding travel speed, surface finish and stress ratio).

Since 2005, the volume of FS weld fatigue data published in various journals and conference proceedings has increased considerably. Thus, in 2015 de Oliveira Miranda et al.[16] published a comprehensive review and statistical analysis of literature data that derived fatigue curves for FS aluminium welds, which then served as a basis for their probabilistic fracture mechanics model[16]. In comparison with the design S-N curves for fusion welds given in the IIW recommendations[14], the S-N curves representing 50% and 97.7% survival probability (with 95% confidence) that were proposed in reference [16] for FS welds, showed a lower inverse slope and a significantly higher fatigue strength. However, compared with the approach in reference [15], the analysis reported in [16] for joints made of 5xxx and 6xxx series, made no distinction by temper condition, surface finish, PWHT or stress ratio (for example, data at R = 0.1 and R = -1 were merged together).

A key difference between fusion welds and those made by a solid state friction stir welding process is the lower level of tensile residual stress that occurs in FS welds. This implies that it is worth re-visiting the assumption that underlies the use of unique geometric category-based S-N curves for fusion welds irrespective of stress ratio, i.e. that the level of residual stress is of yield strength magnitude. In this case the applied stress cycle essentially cycles down from the yield strength no matter what value the nominal applied stress ratio has. By contrast, the lower level of residual stress in FS welds implies that some effect of the stress ratio on the fatigue strength has to be expected. Accordingly, the analysis of experimental data should consider explicitly the stress ratio as a separate factor influencing the fatigue strength.

In the case of FS welds, it therefore seems sensible to follow the approach adopted in reference [15] and adopt a classification system for categorising FS fatigue data for subsequent statistical analysis that allows the effect of individual influential parameters (e.g. alloy type, temper condition, stress ratio, PWHT) to be distinguished and analysed separately. Thus the present paper extends the analysis presented in [15], whilst also incorporating the findings obtained in [16], to develop a set of reference S-N fatigue curves for 97.7% survival probability with a 95% confidence level. These S-N curves are based on a statistical analysis of more than 500 fatigue data for FS welds and include data published since 2005.

The objectives of the work were therefore firstly, to analyse sufficient fatigue data to provide meaningful results and conclusions for engineering designers to use in fatigue design for FS welds and, secondly, to verify whether the categorisation proposed in [15] still applies in the

light of the more recent experimental data. Finally, the paper checks whether such data also fit the fatigue curves proposed in [15]. The proposed set of reference S-N fatigue design curves presented in the present work provide a useful guideline for engineers engaged in the design of FS aluminium welds subject to fatigue loading.

Classification of data

This study collected and analysed experimental fatigue data on nominally defect-free FS welds in 2xxx, 3xxx, 5xxx and 7xxx aluminium alloys in both the naturally and artificially aged conditions. The dataset includes flat plate and small diameter tubular butt-joints with thickness values in the range 2 mm to 13 mm, subjected to constant amplitude uniaxial fatigue loading in laboratory air at various stress ratios (R = -1, 0, 0.1, 0.5). The study also considered the influence on fatigue life of several different post-weld heat and mechanical treatments.

Experimental data was not included for welded joints that were either not butt welds or were made between dissimilar alloys, or that contained macroscopic defects or notches, or that joined plates of different thicknesses. In the data, no specific distinction is made with regard to process parameters, such as tool pin profile, rotational speed and welding speed. It should be emphasised, however, that these process parameters have a direct impact on the weld zone microstructure and, in turn, on the mechanical properties of FS welds[17,18]. Incorrect or sub-optimum process parameters may lead to flawed or defective welds, which will exhibit a reduced fatigue strength compared with nominally defect-free welds, as fatigue cracks initiate from any pre-existing defects[15]. The relationship between defect population and fatigue life reduction was not the focus in the present study, and hence the statistical analysis collected data only from nominally defect-free joints made using optimised process parameters.

Table 1 lists all the data used in the statistical analysis that is discussed below. The set includes about 500 entries, almost 200 more than those collected in [15] (in Table 1 an asterisk identifies new data). Prior to performing a statistical analysis, it was first necessary to classify the data. As can be seen, Table 1 clusters a rather heterogeneous set of data, which differ in terms of parent material, temper conditions, welding parameters, post-welding mechanical or heat treatment, and the stress ratio used in the fatigue tests. This variations would be expected to lead to large differences in fatigue performance, although it is not easy to identify *a priori* which parameters are the most influential in terms of either increasing or decreasing the fatigue strength of the welded joints.

Some trends have emerged from previous studies (see for example [15]) which suggest that fatigue data could be categorised into a certain number of subsets, which then contain FS welded joints with similar fatigue behaviour. Selecting the categorising criteria, however, is a rather critical and complex task, that in the present work was made easier, and was also guided by, principles inferred from the work reported in [15]. The general principle adopted here was to choose categorising criteria that allowed the widest number of subsets to be obtained whilst avoiding the exclusion of factors that may genuinely influence the fatigue strength of FS welds. This requires consideration of issues such as whether welds in 2xxx, 5xxx, 6xxx and 7xxx alloys have comparable fatigue strength values that would allow them to be categorised together, or whether they should be classified into separate categories. It also required consideration of the role of *R*-ratio, and the effect of the temper condition (naturally or artificially aged) on the fatigue strength of welds in heat treatable alloys. On the other hand, certain factors were considered to be relatively insignificant (e.g. thickness, welding process parameters), which then allowed the total number of categories to be kept within a reasonable value.

Based on these premises, the main factors considered when categorising the data were:

- distinction between heat treatable alloys (2xxx, 6xxx and 7xxx series) and strain hardened alloys (in this study, only series 5xxx);
- temper condition: naturally aged (NA) versus artificially aged (AA) conditions;
- stress ratio *R*: to investigate the effect of mean stress;
- post-weld heat treatment or mechanical treatments, e.g. polishing;
- geometry: to include a special class of small diameter tubular joints and which will be referred to as high curvature joints in this paper.

Within heat treatable alloys, the series 7xxx of high strength alloys was further distinguished, as their mechanical properties are generally recognised to be higher than other heat treatable alloys. The set of heat treatable alloys (2xxx, 6xxx in this study) was also classified based on the temper condition.

The overall categorisation system is shown in Table 1 (first column) and Table 2. Each category is labelled by an alphanumeric code, which has 2 to 4 characters. The first letter of the code denotes the type of alloy:

- A – for 5xxx series (≈ 100 data);

- B – for 2xxx and 6xxx series, in T3 or T4 temper condition (~ 200 data);
- C – for 2xxx and 6xxx series, in T5 or T6 temper condition (> 250 data);
- D – for 7xxx series (≈ 20 data);

In second position, a number identifies the value of the stress ratio *R*:

- 0 – for R= 0, 0.1 (values present in all categories, ~ 300 data);
- 1 – for R=-1 (only in categories A and C);
- 5 – for R=0.5 (only in categories B and C);

When necessary, one or two letters are added to specify the post-weld treatment:

- M – for machined joints (this treatment is present in all categories);
- P – for heat treated joints (only for category B);

An additional letter H could also be appended to the code to identify data for tubular joints, i.e. 38 mm diameter tube-on-tube circumferential welds[46], which form two additional categories (C0H, C1H).

To summarise, welded joints in 5xxx alloys subjected to fully-reversed (R=-1) fatigue loading, for example, fall into category A1, while A0 refers to 5xxx series joints tested at R=0. Compared to A1, the category A1M includes only data from specimens where the welds were subjected to post-weld mechanical treatment (e.g. polished or machined) and tested at *R*=-1. As further amplification, consider the data taken from [38], of which around half fall in category A1 (welds not treated) and the other half (welds polished) lie in category A1M. Similarly, category C0 contains data from welds in both 2xxx and 6xxx series alloys, tested at R=0, while the C1 category relates to specimens tested at R=-1 for welds only in the 6xxx series alloys. Note that, in general, each category gathers data from multiple sources, although some exceptions to this statement do exist (e.g. A1, B0MP, D0, D0M, C0H and C1H).

The category and classification coding are summarised in Table 2. Overall, this classification system provides a total of 15 categories, with 4 types of alloys, 4 load ratios, 2 post-weld treatments and one special class of tubular geometry. This classification allows the analysis to discriminate the effect of several influential factors. For example, it provides two separate categories (A, D) for 5xxx series (not heat treatable) and for 7xxx series (high strength alloys). It categorises together the 2xxx and 6xxx alloys, which however are further differentiated based on their temper condition: category B for naturally aged alloys (T3 or T4

temper condition) and category C for artificially aged alloys (T5 and T6 conditions). It also accounts for the effect of mean stress in a fatigue cycle (through stress ratio, *R*) and reserves separate designations for post-weld treated welds (M or P) or tubular joints (H).

Statistical analysis of fatigue data

The nominal stress range, Δσ, and the number of cycles to failure, *N*, were the quantities recorded for each data point in all the bibliographic sources available. Only data with values of cyclic life *N* between 10^3 and 2 x 10^6 were included. Table 1 indicates the number *n* of data points collected from each source manuscript, as well as the total number of points contained in each category. These fatigue data were used to obtain a predicted stress-life (S-N) curve using the Basquin equation $\Delta\sigma^k N = \Delta\sigma_A^k N_A$, where *k* is the inverse slope and $\Delta\sigma_A$ the reference fatigue strength at $N_A = 2 \times 10^6$ cycles. The mean S-N curve, representing a 50% probability of failure, is given on log-log axes, using a linear regression model $y = a + bx + \varepsilon$, where $x = log\Delta\sigma$, $y = logN$ is the transformed stress range and *N* is the number of cycles to failure. For a standard normal distribution of life, the symbol ε denotes a zero mean normally distributed random variable, which accounts for the scatter in experimental data. A log-normal regression model is used in this work as the S-N data is assumed to be homoscedastic, i.e. it describes a situation in which the error term (that is, the "noise" or random disturbance in the relationship between the independent variables and the dependent variable) is the same across all values of the independent variable of stress.

A least-squares fitting of the data provides the estimators of regression parameters $\hat{a}$, $\hat{b}$ and s^2 (which is an estimate of the variance in ε), see Appendix A. In the *x*-*y* diagram, the mean S-N line for a P_s=50% survival probability is $y_{50\%} = \hat{a} + \hat{b}x$, where $y_{50\%} = logN_{50\%}$ relates to the fatigue life $N_{50\%}$ at stress range $x = log\Delta\sigma$. By inverting Eq. (A.1), one obtains the estimates both of the inverse slope *k* and of the reference fatigue strength $\Delta\sigma_{A,50\%}$ for P_s=50% survival probability (symbol ^ is now omitted):

$$k = -\hat{b} \quad ; \qquad \Delta\sigma_{A,50\%} = \left(\frac{10^{\hat{a}}}{N_A}\right)^{\frac{1}{k}} \tag{1}$$

The mean S-N line in the $\Delta\sigma - N$ diagram is given by $\Delta\sigma^k N = \Delta\sigma_{A,50\%}^k N_A$, see Figure 1. A survival probability P_s=50% implies that half of all new or future observations would lie below the mean S-N line (unsafe prediction). For fatigue design purposes, a much higher probability of survival represents the recommended fatigue design curve[14], typically P_s=97.7%, i.e. mean minus two standard deviations. This increased survival probability is

equivalent to a lower allowable fatigue strength $\Delta\widetilde{\sigma}_{\mathrm{A},97.7\%}$, which corresponds to the (1-P_s) percentile of the normal distribution of the fatigue life (see Figure 1). A survival probability of 97.7% implies that 2.3 specimens (from 100 tested at a constant stress range $\Delta\sigma$) might fail at a number of cycles lower than the value N predicted by $\Delta\sigma^k N = \Delta\widetilde{\sigma}^k_{A,97.7\%} N_A$.

When estimating the allowable fatigue strength, it is also necessary to evaluate the uncertainty in the statistical estimators. The relatively limited experimental dataset used in the regression analysis means that the estimators given in equation (1) and thus the mean S-N curve are also subject to a statistical uncertainty. Hence the fatigue strength $\Delta\widetilde{\sigma}_{A,97.7\%}$ derived from the mean S-N curve is affected by statistical uncertainty. A confidence level for the estimated fatigue parameters therefore has also to be quantified[14]. These two considerations require the characteristic (or design) S-N curve[1] to be defined for a high survival probability P_s with confidence γ, that is determined according to the expression given in equation (2):[14,56]

$$y_{(P_s;\,\gamma)} = y_{50\%} - q \cdot s \tag{2}$$

where q is a statistical parameter that establishes the deviation below the mean. In equation (2), $y_{(P_s;\gamma)} = logN_{(P_s;\gamma)}$ relates to the number of cycles to failure $N_{(P_s;\gamma)}$ at stress range $x = log\Delta\sigma$ (for a survival probability P_s and confidence γ), whereas $y_{50\%} = logN_{50\%}$ is the mean fatigue life from the regression line, see Figure 1. In the most general case, the value of q depends on probability P_s and confidence γ, on the stress $x = log\Delta\,\sigma$ at which life $y_{(P_s;\gamma)}$ is calculated, on the number n of specimens tested to failure, as well as the experimental setting defined by the specific values $(\Delta\sigma_i, N_i)$, $i = 1,\ldots, n$ used in experiments[56].

Parameter q can be determined using the tolerance interval approach[14,55]. When q is not constant over the stress range, the design S-N curve is an hyperbola, rather than a straight line, and it has variable distance from the mean regression S-N line (the closest distance being at the mean log-stress value $\bar{x}$, see Eq. (A.3)). Since hyperbolic S-N curves could be laborious to estimate and use in practical applications, a straight line approximation (assuming q = const.) is often preferred, although this involves some loss of confidence level[56]. The statistical analysis in this paper will adopt the model proposed in [15] that is given in equation (3):

[1] The term "design S-N curve" is often used to designate a characteristic S-N curve that is factored by a partial safety factor[14].

$$q = \Phi_{(P_s)}^{-1} + t_{(\gamma;n-2)} \frac{\sqrt{2}}{\sqrt{n-2}} \quad (3)$$

where $\Phi_{(P_s)}^{-1}$ is the P_s-percentile from the inverse standard normal cumulative distribution, $t_{(\gamma;n-2)}$ is the one-tail γ-percentile of Student's *t*-distribution with $(n-2)$ degrees of freedom, and γ is the confidence level (typically taken as γ = 95%). The values of $\Phi_{(P_s)}^{-1}$ and $t_{(\gamma;n-2)}$ are tabulated in statistics textbooks; for example, by choosing P_s = 97.7%, γ = 95% and $n = 10$, their values are $\Phi_{(97.7\%)}^{-1} = 2$ and $t_{(95\%;8)} = 1.860$).

In Eq. (3), *n* is the sample size (number of specimens tested) and $\sqrt{2}$ is a correction factor for small values of *n*, which takes into account the error introduced in the estimation of the variance s^2.[15]

By combining equations (2) and (3), the number of cycles to failure $N_{(97.7\%;95\%)}$ at stress range $x = log\Delta\sigma$, for a survival probability P_s = 97.7% and confidence γ = 95%, is determined as indicated in equation (4):[15]

$$logN_{(97.7\%;\,95\%)} = logN_{50\%} - \left(\Phi_{(97.7\%)}^{-1} + t_{(95\%;\,n-2)} \frac{\sqrt{2}}{\sqrt{n-2}}\right) \cdot s \quad (4)$$

where $N_{50\%}$ is the number of cycles (at stress range $x = log\Delta\sigma$) from the regression line and corresponding to a survival probability of 50%. A confidence of 95% means that, out of 100 predictions given by equation (4), five could be false, i.e. the fatigue life in a new future observation would lie above the estimated value $N_{97.7\%;95\%}$ given by equation (4) at the prescribed probability of 97.7%.

Note that in equation (4) the quantity $logN_{97.7\%} = logN_{50\%} - \Phi_{(97.7\%)}^{-1} \cdot s$ locates the 97.7%-percentile $N_{97.7\%}$ on the log-normal distribution for *N*, which has mean $y_{50\%}$ and variance s^2 estimated by regression analysis. Note that the values $N_{97.7\%}$ at each stress range identify the S-N line characterised by the fatigue strength $\Delta\tilde{\sigma}_{A,97.7\%}$ at N_A cycles, see Figure 1. Instead, the last term in the right hand side, $t_{(0.95\%;n-2)}\frac{\sqrt{2}}{\sqrt{n-2}} \cdot s$, accounts for the confidence to correct the estimated percentile $N_{97.7\%}$.

As the sample size *n* increases (i.e. as $n \to \infty$), the last term in Eq. (4) under the square root ($\sqrt{2/(n-2)}$) decreases and the factor $t_{(0.95\%;n-2)}\frac{\sqrt{2}}{\sqrt{n-2}}$ becomes negligible compared to $\Phi_{(P_s)}^{-1}$. The relative importance can therefore be quantified by the ratio $r = \frac{t_{(0.95\%;n-2)}\ \sqrt{2}}{\Phi_{(P_s)}^{-1}\ \sqrt{n-2}}$, as

a function of the sample size n. For example, for n = 10, r = 0.466, while for larger sample sizes r = 0.290 (n=20), r = 0.194 (n=40) and r = 0.119 (n = 100). Hence $r \to 0$ as $n \to \infty$, which means that for very large sample size the scatter in statistical estimations becomes very low.

Although approximate, the statistical model given in equation (4) provides results that are in very close agreement with the tolerance factor approach for a univariate distribution[56]. This can be confirmed by comparing q in Eq. (3) to the tolerance factor k for a univariate distribution[2], given in Table 1 of [59] for a survival probability P_s = 97.7% and confidence level γ = 90%. For sample sizes $n \geq 5$, the largest difference occurs for n = 7, where q = 1.274 and k = 3.389, with a deviation of –3.5% (the approach given in equation (4) being slightly non-conservative). A smaller deviation occurs for other values of n. Whilst a deviation larger than 6% is observed with a very small sample size (n=3, 4), these low values are of no interest in this paper.

Equation (4) gives the lower bound S-N curve for a survival probability P_s = 97.7% (and 95% confidence), which represents the statistical (mean minus two standard deviations) fatigue design curves usually used in safe-life (S-N) design procedures. The upper bound S-N curve for P_s=2.3% (i.e. mean plus two standard deviations) is symmetrical about the mean line and hence the fatigue life $logN_{2.3\%}$ can simply be obtained by replacing the "+" sign with a "–" sign in equation (4).

The statistical approach that has been summarised above assumes that scatter and confidence level are constant over all stress ranges, which then gives a constant inverse slope k regardless of the assumed probability of failure P_s. Extrapolation of the S-N line at N_A cycles identifies the design fatigue strength $\Delta\sigma_{A,Ps}$. The mean minus two standard deviations design S-N curve given in equation (2), can be written explicitly as $y_{(P_s;\,\gamma)} = \hat{a} + \hat{b}x - q \cdot s$, which is equivalent to $y_{(P_s;\,\gamma)} = \hat{a}_d + \hat{b}x$, where $\hat{a}_d = (\hat{a} - q \cdot s)$ is a new intercept. The inverse slope remains unchanged, because S-N lines are just translated.

This new intercept $\hat{a}_d$ allows the fatigue strength $\Delta\sigma_{A,97.7\%}$ at N_A cycles (for a survival probability 97.7% with a confidence level of 95%) to be computed in a similar fashion to

[2] Note that also the "tolerance factor for univariate distribution" is approximate when applied to regression analysis. The correct approach would be the "tolerance factor for regression", which calculates a variable q factor and, for this reason, it is rather complicated to implement[56].

equation (1), by replacing $\hat{a}$ with $\hat{a}_{\mathrm{d}}$. The fatigue strength $\Delta\sigma_{A,2.3\%}$, equivalent to a failure probability of 2.3%, is obtained by using the intercept $(\hat{a} + q \cdot s)$. Using the value $\Delta\sigma_{A,50\%}$ in equation (1), expressions for the design fatigue strengths at probabilities of survival of P_s=97.7% and 2.3% can easily be obtained (for clarity, the subscript indicating a confidence level of 95% is now omitted):

$$\Delta\sigma_{A,97.7\%} = \Delta\sigma_{A,50\%}\left[10^{-\left(\Phi^{-1}_{(P_S)} + t_{0.95\%}\frac{\sqrt{2}}{\sqrt{n-2}}\right)s}\right]^{\frac{1}{k}}$$

$$\Delta\sigma_{A,2.3\%} = \Delta\sigma_{A,50\%}\left[10^{+\left(\Phi^{-1}_{(P_S)} + t_{0.95\%}\frac{\sqrt{2}}{\sqrt{n-2}}\right)s}\right]^{\frac{1}{k}} \quad (5)$$

In the present paper the statistical scatter in the data will be defined by the band of fatigue strength values falling inside the boundaries of the mean ± two standard deviations lines, and is therefore measured by the parameter $T_\sigma = \Delta\sigma_{A,2.3\%}/\Delta\sigma_{A,97.7\%}$, which on the basis of equation (5) can also be written as $T_\sigma = (10^{+2qs})^{\frac{1}{k}}$. Therefore, T_σ depends on both the sample size n (through factor q) and the standard deviation s (which quantifies the scatter in the experimental data).

Discussion of results

The estimated values of both the inverse slope k and the stress ranges $\Delta\sigma_{A50\%}$, $\Delta\sigma_{A,97.7\%}$, corresponding to a fatigue life of $N_A = 2 \times 10^6$ cycles (for survival probabilities of 50% and 97.7%, with a confidence level of 95%) are listed in the last three columns of Table 1, for each individual set of data. The estimated values for each category of aluminium alloys are summarised in Table 3. The stress range $\Delta\sigma_{A,97.7\%}$ (in MPa) at $N_A = 2 \times 10^6$ is commonly used in design codes (e.g. Eurocodes, IIW) to characterise the fatigue strength of a class of welded detail in safe-life design.

In Figure 2 to 8, the experimental fatigue data for each individual category of alloys are compared with both the mean regression line and the characteristic S-N curves corresponding to probabilities of 2.3% and 97.7% (with a confidence level of 95%), which define the scatter band falling within ± two standard deviations. In all cases examined (except categories C0 in Figure 3(a) and B0M in Figure 4(a)), the data lie within the scatter band.

The statistical dispersion in the experimental data is measured by T_σ values, which are given in the last column of Table 3. It is clear that categories A1M and C5 have the largest values of T_σ and hence the greatest scatter in data, as also seen in Figure 6(b) and Figure 7(b), while category B0MP has the smallest value of T_σ. Figure 9 presents a comparison between the characteristic S-N fatigue design curves (i.e. mean minus two standard deviations representing a 97.7% survival probability) for each individual alloy category. These figures allow the effect of stress ratio, post-weld treatment and tubular specimens (high curvature in the Cxx category) to be clearly observed through the changes in the slope and position of the design S-N curves. Figure 9(d) also shows the Eurocode 9 Class 125 fatigue design curve applicable to the parent plate (base metal) in 7xxx alloys. This will be discussed further in the next Section.

A careful analysis of Table 1 reveals that the new data published since 2005, have fatigue properties that are consistent with those of similar alloys in the same category, as the data published prior to 2005. This commonality reinforces the validity of the categorisation and classification system suggested by [15] and also adopted in this study.
The results summarised in the various figures and tables also support the main conclusions suggested by [15] regarding the effect of some influential parameters (e.g. parent alloy, temper condition, post-weld treatment and stress ratio) on the fatigue behaviour.

Effect of parent material and temper condition
The categorisation system used in this study has classified friction stir welds based on type and mechanical properties of parent alloy. Alloys in the 5xxx series (non-heat treatable) have a separate category, as do the high-strength 7xxx series alloys. For 2xxx and 6xxx series alloys that are heat treatable, the effect of parent alloy is subordinate to the effect of temper condition, thus requiring a distinction to be made between naturally and artificial aged joints.

Considering the fatigue strength data given in Table 3, it is clear that for a stress ratio $R = 0$ (the x0 category) the 7xxx series alloys (category D0) show the highest values of fatigue strength. In fact, the fatigue strength of the D0M category is the highest in the table. In the case of the joints tested at $R = -1$, the data indicate that 5xxx and 6xxx series alloys have very similar fatigue strengths that are approximately 15% higher than those seen for the 7xxx series alloys tested at $R = 0$ (categories A1 and C1 compared with category D0). In category CH1, however, the positive effect of a compressive stress ($R = -1$) is more than offset by the high curvature giving a relatively low value of fatigue strength.

It is also seen from Table 3 that in heat treatable 2xxx and 6xxx series alloys the fatigue strength is largely dominated by the temper condition, i.e. naturally aged (T3 or T4) or artificially aged (T5 or T6), with naturally aged alloys (B0) showing superior fatigue strength to artificially aged alloys (C0). The work presented by [15] also found that temper condition had a significant role in the fatigue performance of FS welds in heat treatable alloys, with natural ageing providing a superior performance compared with artificially aged specimens. A similar trend occurs for joints with post-weld mechanical treatment (categories B0M and C0M).

Effect of post-weld treatment

Since FS welding is a solid-state process, with no liquid/solid phase transformation such as occurs in fusion welding, it usually leads to high quality welds with few internal defects or flaws, provided that tool geometry and process parameters are chosen correctly. Defect-free welds generally still show a fatigue strength below that of parent plate, which then suggests that fatigue behaviour is mainly controlled by crack nucleation at weld surface irregularities, arising particularly at the tool shoulder region where flash may exist[57]. Removing surface profile irregularities results in increased fatigue strength. This has been documented in [1,15, 57] and also confirmed in the present work.

The effect of post-weld machining on the fatigue behaviour can be evaluated by comparing the stress range $\Delta\sigma_{A,97.7\%}$ in Table 3 for categories A1/A1M (series 5xxx), B0/B0M/B0MP (series 2xxx and 6xxx alloys, naturally aged), C0/C0M (series 2xxx and 6xxx alloys, artificially aged) and D0/D0M (series 7xxx alloys), and can be seen to be rather low for the 2xxx and 6xxx series alloys. For instance, the fatigue strength of category B0M is within 4% of that of category B0, while categories C0 and C0M have fatigue strengths that lie within 1% of each other. For the 7xxx series alloys, however, (categories D0 and D0M) post weld machining confers a 32% increase in fatigue strength. In contrast, for the 5xxx series alloys tested at R = -1 (categories A1 and A1M), post-weld machining leads to a 29% decrease in fatigue strength.

This apparent contradiction can be explained by considering the scatter of experimental data. As shown in equation (5), the characteristic stress corresponding to a 97.7% probability of survival, $\Delta\sigma_{A,97.7\%}$, depends on both the average stress $\Delta\sigma_{A,50\%}$ and the scatter band in the S-N data, measured by the standard deviation s through the T_σ parameter. For the same value of

$\Delta\sigma_{A,50\%}$, a larger scatter band, i.e. a larger T_σ, gives a lower value of characteristic stress $\Delta\sigma_{A,97.7\%}$. It may then happen that two S-N curves that have similar values of $\Delta\sigma_{A,50\%}$ but different scatter bands (different T_σ), have markedly different values of $\Delta\sigma_{A,97.7\%}$. Conversely, two S-N curves with similar values of $\Delta\sigma_{A,97.7\%}$ may have, instead, quite different values of $\Delta\sigma_{A,50\%}$.

This explains, for example, why no clear change is observed for $\Delta\sigma_{A,97.7\%}$ in categories B0/B0M, despite the average stress range $\Delta\sigma_{A,50\%}$ increasing by 18% from 125.9 MPa for as-welded joints (category B0) up to 149.2 MPa for machined joints (category B0M). In fact, category B0M has a wider scatter band than B0 (T_σ=2.28 vs. T_σ=1.76). A similar trend is observed with A1/A1M categories, in which machined welds show a surprisingly low characteristic strength (99.02 MPa), compared with as-welded joints (127.37 MPa), in spite of the average stress $\Delta\sigma_{A,50\%}$ increasing by about 6% from 155.47 MPa (A1, as-welded) to 164.51 MPa (A1M, machined).

Some of the large scatter in certain categories may also arise from heterogeneity of the surface conditions in machined welds (including the residual stress level resulting from manufacturing processes). Very few fatigue studies fully characterise the surface condition, despite the fact that fatigue cracks almost invariably start at the surface. As an example of the possible influence of this surface condition effect, it can be noted that data in category A1 for 5xxx series alloys are taken mainly from [38], while those in the A1M category also include data from other sources. However, the work of [38] confirms that there is a significant increase in fatigue strength by surface finishing. The same comments apply to data in categories B0 and B0M taken from references.[24,25,26,28]

Effect of stress ratio

There is a strong influence of mean stress in fatigue and hence of stress ratio on the fatigue strength. This was emphasised in the work by [15]. For example, welded joints in 5xxx series alloys showed an increase in fatigue strength of 68% when tested under fully reversed loading at R = -1, compared with R = 0.1. The data presented in Table 3 confirm this trend. For 5xxx series alloy (category Axx), for example, the fatigue strength increases by approximately 44% from 88.6 MPa (category A0) to 127.4 MPa (category A1). Closer inspection of the data in categories A0 and A1 (see Table 1) indicates that testing at R = -1 always gives a higher fatigue strength than testing at R = 0, with the lowest fatigue strength in the A1 category still being higher than the highest value in category A0.

For FS welds in 2xxx or 6xxx series alloys (category Cxx), the fatigue strength almost doubles as the loading changes from R = 0.5 (fatigue strength 31.2 MPa category C5), through R = 0.1 (category C0 fatigue strength 62.1 MPa) to R = -1 (fatigue strength 123.3 MPa category C1). A 50% increase is also observed in the data for "high curvature joints" (small diameter tubes categories C0H and C1H), where the strength increases from 28.5 MPa (category C0H, R = 0.1) to 56.3 MPa (category C1H, R = -1).

The strong effect of stress ratio arises from the reversed plasticity that occurs during fully reversed loading and that creates a partially compressive residual stress field at the crack tip. It is worth noting that the fusion weld fatigue design codes usually ignore the influence of stress ratio using the rationale that the residual stress at welds is of yield strength magnitude and hence, irrespective of the applied stress ratio, the actual crack tip stress cycles down from yield strength and this is therefore equivalent to a high mean stress value in the fatigue cycling. In the case of solid state friction stir welds where the transverse tensile residual stresses are much lower, it makes sense to incorporate stress ratio as an influencing factor in the design curves.

Effect of high-curvature

Category "xxH" collects data for semi-automatic FS welds made between 38 mm outer diameter 6082-T6 seamless tubes. The development of the welding process is detailed in [45]. To avoid a large hole defect in the joint, the process utilises a retracting pin tool that assures high quality defect-free joints. The fatigue data are taken from [46,47,48,49]. No similar data are available in the literature; other work dealing with FS welds between tubes either used much larger diameters[52], or they focused on technological aspects of welding[53,54].

The data from tests at R = -1 (categories C1 and C1H) show that the reference stress range $\Delta\sigma_{A,97.7\%}$ is almost halved for tubes compared with flat plate specimens, from 123.3 MPa (C1) to 56.3 MPa (C1H). This marked decrease in strength is primarily attributed to the notch effect caused by the slight undercut at the edge of the weld zone arising from the tool shoulder[50,51]. An average notch root radius of about 0.5 mm was measured by [50], on both the advancing and the retreating side of the weld, which led to a local stress concentration factor of 2.4 in axial loading and 1.7 in torsion. Counterbalancing this result is the observation that the fatigue strength of such tube-on-tube welds remains comparable to that of their fusion weld counterparts.

Comparison with Eurocode 9

Eurocode 9 (EC9) provides design Δσ-N curves for a variety of plain members, welded attachments, and members with longitudinal or transverse welds. The curves are identified by a constant amplitude stress range $\Delta\sigma_C$ at $NA = 2 \times 10^6$ cycles (the reference fatigue strength) and the inverse slope m_1. For constant amplitude fatigue loading, a fatigue limit $\Delta\sigma_D$ is taken at 5×10^6 cycles, below which constant amplitude stress cycles are assumed to be non-damaging. Each S-N design curve represents the mean line minus 2 standard deviations, which gives a survival probability of 97.7%. The detail category depends on several factors that include constructional detail, initiation site, weld type (e.g. full penetration but weld ground flush), and the type of welding (e.g. continuous automatic welding).

The fatigue curves in EC9 are applicable only to aluminium joints made using arc welding (metal inert gas and tungsten inert gas) and therefore cannot, at present, be applied to friction stir welds. It is also the case that no other standard currently exists for fatigue design of friction stir welds. With this in mind, the aim of the present work is to provide a quantitative comparison with existing standards and hence the reference fatigue curves obtained in this study are compared with the design S-N curves provided in EC9 for arc welding. The objective is determination of the appropriate design category for friction stir butt welds in aluminium alloys. Detail categories for comparative purposes are selected for plain material and full penetration butt welds from Annex J in EC9 as:

- Base metal (for plain geometry, with surface finish R_{z5}<40 μm, visual inspection):
    - $\Delta\sigma_C$=125 MPa, m_1=7 (Category 125-7 the highest plain material category applicable to 7020 only);
    - $\Delta\sigma_C$=90 MPa, m_1=7 (Category 90-7 the highest plain material category applicable to other alloys);
- Butt weld (flat geometry, quality level B as per EN ISO 10042:2005):
    - $\Delta\sigma_C$=56 MPa, m_1=7 (Category 56-7 welded both sides, caps ground flush both sides, crack initiation in weld);
    - $\Delta\sigma_C$=50 MPa, m_1=4.3 (Category 40-4,3 full penetration welded from both sides, crack initiation at weld toe);
- Butt weld (hollow, tubular, quality level C as per EN ISO 10042:2005):
    - $\Delta\sigma_C$=32 MPa, m_1=3.4 (Category 32-3,4 welded from one side only without backing, crack initiation at weld toe)

A comparison that plotted in a single figure all the S-N curves for the various categories listed in Table 3 would be rather cluttered. It is therefore preferable to present only some representative results in separate figures, as follows:

- Figure 9(d) - the proposed design S-N curves for FS welds in 7xxx series alloys for both as-welded and surface machined conditions (Dxx) compared with the EC9 curves for the 7xxx base metal class
- Figure 10(a) - the proposed design S-N curves for 5xxx series alloys (Axx), and for 2xxx and 6xxx series alloys in the naturally (Bxx) and artificially (Cxx) aged conditions, compared with the EC9 curves for base metal (other than 7xxx series) and for butt joints in as-welded and machined conditions.
- Figure 10(b) - the proposed design S-N curves for 2xxx and 6xxx series alloys in the artificially aged condition (Cxx), compared with the EC9 curves for the previous case.
- Figure 10(c) - the proposed design curves for high curvature tube-on-tube joints (CxxH) compared with the EC9 curves for tubular joints.

As mentioned earlier, the S-N curves reported in EC9 refer to fatigue data obtained at relatively high mean stress (stress ratio $R \geq 0.5$).[60] Hence, for the case of friction stir welds, almost all the curves for $R = 0$ and 0.1 (categories xx0) are collected together in Figure 10(a) (category A1 is an exception added for comparative purposes). The curves for other R ratios are shown in Figure 10(b), while curves for tube-on-tube high curvature joints are compared in Figure 10(c). Fatigue curves for machined welds are not shown, since they are positioned above those shown in Figure 10. The effect of natural or artificial aged conditions can be seen in Figure 10(a). On the basis of the available data, Figure 9(d) shows that friction stir welds in the as-welded condition have a fatigue performance close to that of the parent plate in 7xxx series alloys. It should be noted that this is a preliminary result as the categories D0 and D0M show results only for 7475-T76 alloy, from one reference only[24], and further data would be required to validate this preliminary conclusion.

In Figure 10(a), over the range of fatigue lives in the figure, the proposed design curves for FS welds in the 5xxx, 2xxx and 6xxx natural aged alloys (Categories A0 and B0) all lie just above the parent plate Category 90-7 curve from EC9, while the proposed design curve for category A1 is even higher. Therefore, compared to fusion butt joints, FS welds generally show a superior fatigue performance.

In the case of the artificially aged condition, Category C0, the 2xxx and 6xxx FS welds have a steeper slope to their proposed fatigue design curve, giving a fatigue strength at 2 x 10^6 cycles lower than the Category 90-7 parent plate curve from EC9 and more comparable to fusion butt joints. Figure 10(b) illustrates the marked influence of stress ratio on both fatigue strength and on slope of the proposed fatigue design curves for FS welds. Finally, Figure 10(c) shows that at 2×10^6 cycles the proposed fatigue design curve for high curvature FS joints tested at R = -1 is significantly higher than the Category 32-3,4 curve from EC 9. Again, the strong influence of stress ratio can be seen as the joints tested at R = 0.1 have a lower fatigue strength than the Category 32-3,4 curve.

Conclusions

This paper has provided an overview of the fatigue performance for FS joints in aluminium alloys through a statistical analysis of a large set of data drawn from the literature and from work done by the authors. The starting point for the work was the database analysed in by [15] which has been updated with more than 200 additional fatigue results taken from papers published in the open literature since 2005.

The intention in the present work was to access the widest possible database of FS weld fatigue data and then use it to estimate reference S-N fatigue design curves for FS welds in a number of aluminium alloys in various temper conditions and under several values of stress ratio in the fatigue cycling. The available data were organised into a number of different categories, based on the classification criteria suggested by [15]. This allows the fatigue strength to be explicitly correlated to several influential factors (type of alloy, temper condition, surface condition, stress ratio). Aluminium alloys in the 5xxx and 7xxx series were assigned to separate categories, while 2xxx and 6xxx series were grouped together by either natural or artificial aging. The different R ratios used in fatigue testing were also explicitly considered by separate categories.

The reference S-N fatigue design curves for survival probabilities of 50% and 97.7% (at the lower 95% confidence limit) were then estimated for each individual data source, as well as for each category. The additional fatigue data were shown to fit the S-N curves already presented in [15]. The reference S-N curves were systematically compared in order to detect correlations between fatigue properties and some of the influential factors mentioned above. The resulting curves from the statistical analysis of the available data were finally compared

to those given in Eurocode 9 fatigue design codes for fusion welded aluminium alloys. The data confirmed a number of conclusions reached by [15], namely:

1. Temper condition in 2xxx and 6xxx alloys has a marked influence on the fatigue strength, with FS welds in the natural aged condition showing a better fatigue strength than artificially aged alloys.

2. Post-weld machining of the surface confers an increase in fatigue strength. This has been observed, in particular, by comparing the fatigue strength of data taken from the individual sources.

3. In 7xxx series alloys friction stir welds in the as-welded condition have a fatigue performance close to that of the parent plate.

4. There is a marked influence of stress ratio on both fatigue strength and on slope of the proposed fatigue design curves for FS welds.

5. There is some variation in scatter of the experimental data. As shown in equation (5), the characteristic stress corresponding to a 97.7% probability of survival, $\Delta\sigma_{A,97.7\%}$, depends on both the average stress $\Delta\sigma_{A,50\%}$ and the scatter band in the S-N data, measured by the standard deviation s through the T_σ parameter. For the same value of $\Delta\sigma_{A,50\%}$, a larger scatter band, i.e. a larger T_σ, gives a lower value of characteristic stress $\Delta\sigma_{A,97.7\%}$. It may then happen that two S-N curves that have similar values of $\Delta\sigma_{A,50\%}$ but different scatter bands (different T_σ), have markedly different values of $\Delta\sigma_{A,97.7\%}$. Conversely, two S-N curves with similar values of $\Delta\sigma_{A,97.7\%}$ may have, instead, quite different values of $\Delta\sigma_{A,50\%}$.

6. Fatigue data from FS welds joining small diameter tubes (38 mm) shows a decrease of fatigue strength compared to joints in flat plate. This was attributed to the notch effect caused by the slight undercut at the edge of the thermos-mechanically affected weld zone, i.e. at the tool shoulder[46]. However, such joints still have a strength almost comparable to that of their fusion welded counterparts.

7. The comparison with the S-N fatigue design curves given in Eurocode 9 shows that the fatigue strength of FS welded joints approaches that of the parent plate alloy.

8. The overall conclusion from this review and statistical analysis of fatigue data for FS welds is that FSW joints have fatigue strength values generally significantly higher than the values recommended by current fusion weld standards, e.g. Eurocode 9 or IIW.

Appendix A – Estimators of regression parameters

In the regression analysis, a log-transformation is applied to the S-N equation $\Delta\sigma^k N = \Delta\sigma_A^k N_A$ to obtain the linear model $y = a + bx + \varepsilon$, where:

$$a = \log(\Delta\sigma_A^k N_A) \qquad b = -k \tag{A.1}$$

and $x = log_{10}\Delta\sigma$, $y = log_{10}N$ are, respectively, the (transformed) stress range and number of cycles to failure. The normally-distributed random variable ε is added to the regression model to account for the scatter in experimental data.

Assume now that a set of n data $(\Delta\sigma_i, N_i)$, i=1,…,n is available from experimental tests. Apply a log-transformation $x_i = log_{10}\Delta\sigma_i$, $y_i = log_{10}N_i$ to translate the data into the pairs (x_i, y_i) i=1,…, n in the x-y diagram.

The maximum likelihood (least-squares) estimators of the regression parameters a, b are[58]:

$$\hat{a} = \bar{y} - \hat{b}\bar{x} \qquad \hat{b} = \frac{\sum_{i=1}^{n}(x_i - \bar{x})(y_i - \bar{y})}{\sum_{i=1}^{n}(x_i - \bar{x})^2} \qquad s^2 = \frac{1}{n-2}\sum_{i=1}^{n}\left[y_i - (\hat{a} + \hat{b}\,x_i)\right]^2 \tag{A.2}$$

where:

$$\bar{x} = \frac{1}{n}\sum_{i=1}^{n} x_i \quad ; \quad \bar{y} = \frac{1}{n}\sum_{i=1}^{n} y_i \tag{A.3}$$

are the sample mean of the n values x_i, y_i, while s^2 is the unbiased estimator of the variance $Var(\varepsilon)$ of the random variable ε in the regression model. Parameter s^2 gives a measure of the scatter of experimental data around the best-fit mean line $\hat{y} = \hat{a} + \hat{b}x$.

References

1. Lohwasser D, Chen Z. Introduction. In: Lohwasser D, Chen Z, eds. Friction stir welding. From basics to applications, Woodhead Publishing Ltd., Cambridge, UK; 2010:1-12.
2. Hattingh DG, von Wielligh L, Thomas W, James MN. Friction processing as an alternative joining technology for the nuclear industry. *J South African Inst of Mining Metall.* 2015;115(10):903-912.
3. James MN, Bradley GR, Lombard H, Hattingh DG. The relationship between process mechanisms and crack paths in friction stir welded 5083-H321 and 5383-H321 aluminium alloys. *Fatigue Fract Engng Mater Struct.* 2005;28:245-256.
4. Hattingh DG, Blignault C, van Niekerk TI, James MN. Characterization of the influences of FSW tool geometry on welding forces and weld tensile strength using an instrumented tool. *J Mats Proc Technol.* 2008;203(1-3):46-57.
5. Astarita A, Squillace A, Nele L. Mechanical characteristics of welded joints of aluminum alloy 6061 T6 formed by arc and friction stir welding, *Met Sci Heat Treat.* 2016;57(9–10):1-6.
6. Ranes M, Kluken AO, Midling OT. Fatigue properties of as welded AA6005 and AA6082 aluminium alloys in T1 and T5 temper condition. In: Fourth International Conference on Trends in Welding Research, Gatlinburg, TN, USA, 1995:639-44.
7. Haagensen PJ, Midling OT, Ranes M. Fatigue performance of friction stir butt welds in a 6000 series aluminum alloy. In: Computer Methods and Experimental Measurements for Surface Treatment Effects II, 7-9, Milan, Italy; 1996:225–37.
8. Caruso S, Campanella D, Candamano S, Varrese C, Crea F, Filice L, Umbrello D. Experimental comparison of the MIG and Friction Stir Welding processes for AA 6005 Aluminium Alloy. *Key Eng Mater.* 2015;651-653:1480-1486.
9. Shaari MR, Hussain Z, Almanar IP, Van Thuong N. Comparison of Friction Stir and Tungsten Inert Gas weldments of AA6061-T6. *Advanced Materials Research*. 2014;858:19-23.
10. Dickerson TL, Przydatek J. Fatigue of friction stir welds in aluminium alloys that contain root flaws. *Int J Fatigue*. 2003;25:1399–409.
11. ECCS, "European recommendations for aluminium alloy structures", European convention for constructional steelwork, Document No. 68, ECCS, Brussels (1992).
12. EN 1993-1-9:2005 Eurocode 3: Design of steel structures - Part 1-9: Fatigue.
13. EN 1999-1-3:2007/A1:2011 Eurocode 9: Design of aluminium structures - Part 1-3: Structures susceptible to fatigue.
14. Hobbacher A.F. Recommendations for fatigue design of welded joints and components. Second edition. IIW document IIW-2259-15, 2016.
15. Lomolino S, Tovo R, Dos Santos J. On the fatigue behavior and design curves of friction stir butt-welded Al alloys. *Int J Fatigue.* 2005;27:305-316.
16. de Oliveira Miranda AC, Gerlich A, Walbridge S. Aluminum friction stir welds: Review of fatigue parameter data and probabilistic fracture mechanics analysis. *Eng Fract Mech.* 2015;147:243–260.
17. Lombard H, Hattingh DG, Steuwer A, James MN. Optimising FSW process parameters to minimise defects and maximise fatigue life in 5083-H321 aluminium alloy. *Eng Fract Mech.* 2008;75 (3-4):341-354.
18. Krasnowski K, Hamilton C, Dymek S. Influence of tool shape and weld configuration on microstructure and mechanical properties of the Al 6082 alloy FSW joints. *Arch Civil Mech Eng*. 2015;15:133–41.
19. Tovo R, De Scisciolo R, Volpone M. Proprietà Meccaniche e Microstrutturali di Giunti "Friction Stir Welded" in Lega d'Alluminio. In: Proc. of the XXIX National Congress of Italian Association of Stress Analysis (AIAS), 6-9 September 2000, Lucca, Italy, 2000:397-406 (in Italian).

20. Dawes C, Thomas W. Friction stir welding of aluminium alloy. TWI reprint 493/6/95, Bulletin 6, November/December 1995.
21. Pocaterra C, Tovo R. Proprietà meccaniche di giunti testa a testa FSW: stato dell'arte delle leghe leggere e analisi sperimentale su leghe AA5xxx. Degree thesis in Materials Engineering (supervisor: R. Tovo), University of Ferrara, Italy, 2002 (in Italian);
22. Dalle Donne C, Biallas G. Fatigue and fracture performance of friction stir welded 2024-T3 joints. In: Proc. of European Conference on Spacecraft structures, materials and mechanical testing, Braunschweig, Germany, 4-6 November 1998. Paris: European Space Agency (ESA), ESA-SP, Vol. 428, 1999, ISBN: 9290927127:309-314.
23. Biallas G, Dalle Donne C, Juricic C. Monotonic and cyclic strength of friction stir welded aluminium joints. In: Miannay D, Costa P, François D, editors. Advances in mechanical behaviour, plasticity and damage. Proc. of EUROMAT 2000, vol. 1, Amsterdam: Elsevier; 2000:115-20.
24. Magnusson L, Kallman L. Mechanical properties of friction stir welds in thin sheet of aluminium 2024, 6013 and 7475. In: Proc. of Second Int Symposium on FSW, Gothenburg, Sweden, June 2000.
25. Ali A, An X, Rodopoulos CA, Brown MW, O'Hara P, Levers A, Gardiner S. The effect of controlled shot peening on the fatigue behaviour of 2024-T3 aluminium friction stir welds. *Int J Fatigue*. 2007;29:1531-1545.
26. Vidal C, Infante V, Vilaça P. Assessment of improvement techniques effect on fatigue behaviour of friction stir welded aerospace aluminium alloys. *Procedia Engineering*. 2010;2:1605-1616.
27. Franchim AS, Fernandez FF, Travessa DN. Microstructural aspects and mechanical properties of friction stir welded AA2024-T3 aluminium alloy sheet. *Mater Des*. 2011;32:4684–4688.
28. Ghidini T, Dalle Donne C, Alfaro Mercado U. Predicting the fatigue life of pristine and pre-corroded friction stir welded joints". *Int J Structural Integrity*. 2011;2(2):200- 213.
29. Braun R, Biallas G, Dalle Donne C, Staniek G. Characterisation of mechanical properties and corrosion performance of friction stir welded AA6013 sheet. In: Winkler P-J, editor. Materials for transportation industry EUROMAT '99, vol. 1. Wiley–VCH; 2000:150–5.
30. Kawasaki T, Makino T, Todori S, Takai H, Ezumi M, Ina Y. Application of friction stir welding to the manufacturing of next generation 'A-train' type rolling stock. In: Proc of Second Int Symposium on FSW, Gothenburg, Sweden, June 2000.
31. Okura I, Naruo M, Vigh LG, Hagisawa N, Toda H. Fatigue of aluminium deck fabricated by friction stir welding. In: Proc of Eighth Int Conference INALCO 2001, 2001.
32. Dalle Donne C, Raimbeaux G, Biallas G, Allehaux D, Palm F, Ghidini T. Fatigue properties of friction stir welded aluminium butt joints. In: ICAF 2003 - Fatigue of aeronautical structures as an engineering challenge, 2003.
33. Kainuma S, Katsuki H, Iwai I, Kumagai M. Evaluation of fatigue strength of friction stir butt-welded aluminum alloy joints inclined to applied cyclic stress. *Int J Fatigue*. 2008;30:870–876.
34. Cavaliere P, Squillace A, Panella F. Effect of welding parameters on mechanical and microstructural properties of AA6082 joints produced by friction stir welding. *J Mater Process Technol*. 2008;200(1-3):364–372.
35. Sun G, Niu J, Wang D, Chen S. Fatigue experimental analysis and numerical simulation of FSW joints for 2219 Al–Cu alloy. *Fatigue Fract Eng Mater Struct*. 2015;38(4):445–455.
36. Okada T, Suzuki M, Miyake H, Nakamura T, Machida S, Asakawa M. Evaluation of crack nucleation site and mechanical properties for friction stir welded butt joint in 2024-T3 aluminum alloy. *Int J Adv Manuf Technol*. 2010;50:127– 135.
37. Lohwasser D. Thin section airframe alloy welding within WAFS. *Materials Science Forum*. 2003;426-432:2879-2884.
38. James MN, Hattingh DG, Bradley GR. Weld tool travel speed effects on fatigue life of friction stir welds in 5083 aluminium. *Int J Fatigue*. 2003;25:1389–98.

39. Uematsu Y, Tokaji K, Shibata H, Tozaki Y, Ohmune T. Fatigue behaviour of friction stir welds without neither welding flash nor flaw in several aluminium alloys. *Int J Fatigue*. 2009;31:1443–1453.
40. Hagstrom J, Sandström R. Mechanical properties of welded joints in thin walled aluminium extrusions. *Science Technol of Weld Joining.* 1997;2(5):199- 208.
41. Sano Y, Masaki K, Gushi T, Sano T. Improvement in fatigue performance of friction stir welded A6061-T6 aluminum alloy by laser peening without coating. *Mater Des.* 2012;36:809–814.
42. Ericsson M, Sandström R. Fatigue of friction stir welded AlMgSi-Alloy 6082. *Materials Science Forum.* 2000;331-7:1787-1792.
43. Ericsson M, Sandström R. Influence of welding speed on the fatigue of friction stir welds and comparison with MIG and TIG. *Int J Fatigue.* 2003;25:1379–87.
44. Maddox SJ. Review of fatigue assessment procedures for welded aluminium structures. *Int J Fatigue*. 2003;25:1359–1378.
45. Hattingh DG, von Welligh LG, Bernard D, Susmel L, Tovo R, James MN. Semiautomatic friction stir welding of 38 mm OD 6082-T6 aluminium tubes. *J Mater Process Tech*. 2016;238:255-266.
46. Maggiolini E, Tovo R, Susmel L, James MN, Hattingh DG. Crack path and fracture analysis in FSW of small diameter 6082-T6 aluminium tubes under tension–torsion loading. *Int J Fatigue*. 2016;92(Part 2):478–487.
47. Tovo R, Susmel L, James MN, Hattingh DG, Maggiolini E. Crack initiation and propagation paths in small diameter FSW 6082-T6 aluminium tubes under fatigue loading. *Frattura ed Integrità Strutturale.* 2016;10(36):119-129.
48. Hattingh DG, James MN, Susmel L, Tovo R. Fatigue behaviour of Al 6082-T6 friction stir welded tubular joints under torsional loading. *Key Eng Mater*. 2015;627:193-196.
49. Hattingh DG, James MN, Susmel L, Tovo R. Multiaxial fatigue of aluminium friction stir welded joints: Preliminary results. *Frattura ed Integrità Strutturale*. 2015;9(33):382-389.
50. Susmel L, Hattingh DG, James MN, Maggiolini E, Tovo R. Designing aluminium friction stir welded joints against multiaxial fatigue. *Frattura ed Integrità Strutturale*. 2016;10(37):207-214.
51. Susmel L, Hattingh DG, James MN, Tovo R. Multiaxial fatigue assessment of Friction Stir Welded tubular joints of Al 6082-T6. *Int J Fatigue*. 2017;101(2):282-296.
52. Lammlein DH, Gibson BT, DeLapp DR, Cox C, Strauss AM, Cook GE. Friction stir welding of small diameter pipe: an experimental and numerical proof of concept for automation and manufacturing. *Proc Inst Mech Eng, Part B: J Eng Manuf*. 2012;226(3):383–98.
53. Pietras A, Węglowska A, Rams B, Węglowski M. New friction welding technology for joining tubes with lids. *Welding Int.* 2015;30(2):112–118.
54. D'Urso G, Longo M, Giardini C. Microstructure and mechanical properties of Friction Stir Welded AA6060-T6 tubes. *Key Eng Mater*. 2013;554-557:977-984.
55. ISO 12107. Metallic materials - Fatigue testing - Statistical planning and analysis of data.
56. Shen CL, Wirsching PH, Cashman GT. Design curve to characterize fatigue strength. *J Eng Mater Technol-Trans. ASME*. 1996;118:535-541.
57. Dos Santos J, Olea CAW, Coelho RS, Kostka A, Paglia CS, Ghidini T, Dalle Donne C. Metallurgy and weld performance in friction stir welding. In: Lohwasser D, Chen Z, eds. Friction stir welding. From basics to applications, Woodhead Publishing Ltd., Cambridge, UK; 2010:1-12.
58. Wirsching PH, Hsieh S. Linear model in probabilistic fatigue design. *J Eng Mech Div-ASCE*. 1980;106(EM6):1265-78.
59. Schneider CRA, Maddox SJ. Best practice guide on statistical analysis of fatigue data. Doc. IIW-XIII-WG1-114-03, 2003.
60. Maljaars J, Lukić M., Soetens F. Comparison between the Eurocode for fatigue of steel structures, EN 1993-1-9, and the Eurocode for fatigue of aluminium structures, EN 1999-1-3. *Procedia Engineering*. 2013;66:34-48.

FIGURE CAPTIONS

Figure 1. Mean S-N curve from the regression analysis and the design S-N curve at the prescribed probability P_s of survival (97.7%) and confidence γ (95%).

Figure 2. Fatigue curves for FS welds: (a) 5xxx series (category A0); (b) 2xxx and 6xxx series alloys naturally aged (category B0).

Figure 3. Fatigue curves for FS welds: (a) 2xxx and 6xxx series alloys artificially aged (category C0); (b) 7xxx series (category D0).

Figure 4. Fatigue curves for FS welds in 2xxx and 6xxx alloys (naturally aged): (a) machined welds (category B0M); (b) machined and post-weld treatment (category B0MP); (c) post-weld treatment (category B5P).

Figure 5. Fatigue curves for FS welds: categories: (a) 2xxx and 6xxx series alloys naturally aged, machined weld (category C0); (b) 7xxx series, machined weld (category D0M).

Figure 6. Fatigue curves for FS welds in 5xxx series alloys, tested at R=-1: (a) as welded (category A1); (b) machined (category A1M).

Figure 7. Fatigue curves for FS welds in 2xxx and 6xxx series alloys, artificially aged: (a) tested at R=-1 (category C1); (b) tested at R = 0.5 (category C5).

Figure 8. Fatigue curves for high curvature FS welds in 6xxx series, artificially aged: (a) tested at R = 0.1 (category C0H); (b) tested at R = -1 (category C1H).

Figure 9. Comparison of fatigue curves (survival probability P_s=97.7%, confidence 95%) for each category A, B, C and D (for category D, the EC9 S-N design curves are also shown).

Figure 10. Comparison of the fatigue design S-N curves for fusion welds (extracted from EC9) and for friction stir welds (with survival probability P_s=97.7% and lower confidence 95%) for series 5xxx, and 2xxx and 6xxx series alloys in the natural or artificial aged conditions, and for tube-on-tube high curvature joints.

Table 1. Fatigue data used in the analysis presented in the present paper, categorised by alloy type and weld treatment (first column). An asterisk marks the new data added to the original set given by [15].

Category	Ref.	Material	Th. (mm)	rpm/wts	R	No. of data	No. data in each category	k	$\Delta\sigma_{A,50\%}$	$\Delta\sigma_{A,97.7\%}$
A0	[19]	5083-H321	6		0.1	8	34	4.45	100.62	81.03
	[20]	5083-O	6		0.1	9		7.53	126.66	100.27
	[21]	5083-H321	5	/450	0.1	9		5.77	115.86	92.74
	[21]	ALUSTAR-H321	5	/350	0.1	8		4.40	96.15	68.05
B0	[22]	2024-T3 tool B	4	1250/125	0.1	6	89	7.87	172.52	151.77
	[22]	2024-T3 tool B	4	800/80	0.1	6		8.21	165.08	152.11
	[22]	2024-T3 tool A	4	1000/100	0.1	11		6.08	124.08	100.26
	[22]	2024-T3 tool B	4	1000/100	0.1	4		6.84	152.58	132.18
	[23]	2024-T3	1.6	1200/120	0.1	3		6.02	153.02	72.21
		2024-T3	1.6	1800/180	0.1	4		6.21	166.50	135.17
		2024-T3	1.6	2400/240	0.1	4		6.43	178.95	159.23
	[24]	2024-T3	2	1180/110	0.1	9		5.95	147.22	129.51
	[25]*	2024-T3	13	200/120	0.1	9		5.36	152.9	124.36
	[26]*	2024-T351	4	1000/308	0	5		4.38	116.66	95.37
	[27]*	2024-T3	1.6	/700	0.1	21		6.16	132.48	114.58
	[28]*	2024-T3	4	850/300	0.1	7		5.77	144.81	124.09
C0	[20]	2014A-T6	6		0.1	8	124	3.22	93.62	47.77
	[24]	6013-T6	1.6	2000/208	0.1	9		7.05	134.83	110.18
	[29]	6013-T6	4		0.1	11		3.49	72.19	58.94
	[30]	A6N01-T5	–		0.1	12		10.73	104.69	90.35
	[31]	A6N01S-T5	12		0.1	9		6.73	107.22	94.35
	[32]	AA6013-T6	4		0.1	14		3.43	70.68	57.5
	[33]*	A6N01S-T6 0°	10	1500/150	0.1	7		6.30	103.06	90.00

		A6N01S-T6 30°	10	1500/150	0.1	4		8.01	111.7	89.61
		A6N01S-T6 60°	10	1500/150	0.1	4		8.09	114.66	78.97
		A6N01S-T6 90°	10	1500/150	0.1	5		6.66	114.56	89.11
	[34]*	6082-T6	4	1600/40	0.1	9		5.26	114.1	97.24
		6082-T6	4	166/56	0.1	7		10.39	144.62	132.96
		6082-T6	4	1600/80	0.1	8		9.13	132.18	120.4
		6082-T6	4	1600/115	0.1	6		10.15	152.37	133.84
	[35]*	2219-T6	6	800/180	0.1	11		6.74	131.71	113.53
D0	[24]	7475-T76	2	950/110	0.1	10	10	6.86	155.18	113.02
B0M	[24]	2024-T3 milled	2	1180/110	0.1	8	36	12.55	218.19	178.54
	[25]*	2024-T3 mirror polished	13	200/120	0.1	5		8.16	207.89	107.02
	[26]*	2024-T351 smoothed	4	1000/308	0	6		7.52	182.99	166.19
	[36]*	2024-T3 ground	1.6		0.1	6		3.74	108.71	80.13
	[36]*	2024-T3 ground polished	1.6		0.1	3		–	–	–
	[28]*	2024-T3 polished	4	850/300	0.1	8		10.57	226.67	175.34
C0M	[24]	6013-T6 milled	1.6	2000/208	0.1	9	50	10.54	172.15	146.18
	[29]	6013-T6 smoothed	4		0.1	6		6.96	152.60	123.27
	[32]	6013-T6 polished	4		0.1	6		5.78	133.51	79.23
	[37]	6056-T6 milled anodised	4		0.1	12		9.29	144.38	50.28
	[33]*	A6N01S-T6 0° ground	10	1500/150	0.1	6		6.79	112.16	97.54
		A6N01S-T6 30° ground	10	1500/150	0.1	5		3.28	83	69.36
		A6N01S-T6 60° ground	10	1500/150	0.1	3		3.30	82.42	32.79
		A6N01S-T6 90° ground	10	1500/150	0.1	3		10.60	130.46	112.26
D0M	[24]	7475-T76 milled	10	950/110	0.1	8	8	7.41	193.93	143.98
B0MP	[37]	6056-T4 -T6 milled anodised	4		0.1	7	7	10.19	173.47	148.63
A1	[38]	5083-H321	8	500/80	-1	9	36	9.27	185.52	141.96
		5083-H321	8	500/95	-1	8		5.78	156.37	110.42
		5083-H321	8	500/130	-1	8		6.56	153.81	125.87

		5083-H321	8	500/200	-1	11		6.46	161.18	140.20
A1M	[38]	5083-H321 polished	7.4	500/80	-1	8	35	12.85	229.30	180.19
		5083-H321 polished	7.4	500/95	-1	7		3.32	159.31	44.74
		5083-H321 polished	7.4	500/130	-1	6		5.68	186.72	142.91
		5083-H321 polished	7.4	500/200	-1	9		10.71	227.82	191.04
	[39]*	5083-O machined	4	2400/200	-1	5		12.74	316.48	239.78
C1	[31]	A6N01S-T5	12		-1	8	24	8.61	181.04	159.39
	[40]	6082-T5	–		-1	5		4.97	146.65	80.79
	[41]*	6061-T6	3	1400/41	-1	11		8.70	182.18	131.17
C5	[42]	6082-T6	5.8	1000/350	0.5	12	44	4.93	80.87	70.42
	[43]	6082-T6	4	2500/1400	0.5	11		4.49	63.09	50.30
		6082-T6	4	220/700	0.5	14		3.44	58.65	48.07
	[44]	6082-T5	5		0.5	7		5.51	56.34	52.54
B5P	[42]	6082-T4 PWAT	5.8	1000/350	0.5	12	36	3.97	68.64	56.69
	[43]	6082-T4 PWAT	4	2200/700	0.5	11		2.43	49.87	34.29
		6082-T4 PWAT	4	2500/1400	0.5	13		2.96	55.82	42.86
C0H	[46]*	6082-T6	3	800/50	0.1	8	8	4.36	42.16	28.48
C1H	[46]*	6082-T6	3	800/50	-1	6	6	6.46	75.87	56.25

Table 2. Summary of categorisation system and classification coding.

Coding					Material Details	Load ratio
Alloy category	Load ratio	Post welding machining	Post welding ageing	High curvature joints		
A	0				5xxx	0.1
B	0				2xxx and 6xxx naturally aged (NA)	0; 0.1
C	0				2xxx and 6xxx artificially aged (AA)	0.1
D	0				7xxx	0.1
B	0	M			NA milled or smoothed	0; 0.1
C	0	M			AA milled or smoothed	0; 0.1
D	0	M			7xxx milled	0.1
B	0	M	P		NA PWHT milled or smoothed	0.1
A	1				5xxx	-1
A	1	M			5xxx milled or smoothed	-1
C	1				AA	-1
C	5				AA	0.5
B	5		P		NA PWHT	0.5
C	0			H	high curvature	0.1
C	1			H	high curvature	-1

Table 3. Statistical analysis results for the various categories.

Category	No. of data*	k	$\Delta\sigma_A$ (at N=2×10^6 cycles)			T_σ
			50%	97.7% (conf. 95%)	2.3% (conf. 95%)	
A0	32	5.02	107.73	88.63	130.93	1.48
B0	85	4.77	125.95	94.96	167.04	1.76
C0	114	3.86	88.64	62.12	126.49	2.04
D0	9	5.58	137.63	111.99	169.13	1.51
B0M	35	4.63	149.22	98.84	225.29	2.28
B0MP	6	8.70	163.45	138.02	193.57	1.40
C0M	41	3.43	92.69	62.84	136.71	2.18
D0M	8	7.41	193.93	147.68	254.66	1.72
A1	30	5.85	155.47	127.37	189.77	1.49
A1M	30	3.83	164.51	99.02	273.33	2.76
C1	24	6.69	166.59	123.30	225.06	1.83
C5	40	2.55	50.68	31.20	82.32	2.64
B5P	35	2.92	57.29	44.09	74.46	1.69
C0H	8	4.36	42.16	28.48	62.41	2.19
C1H	6	6.46	75.87	56.25	102.34	1.82

* only fatigue points that fall within $10^4 – 2 \times 10^6$ cycles

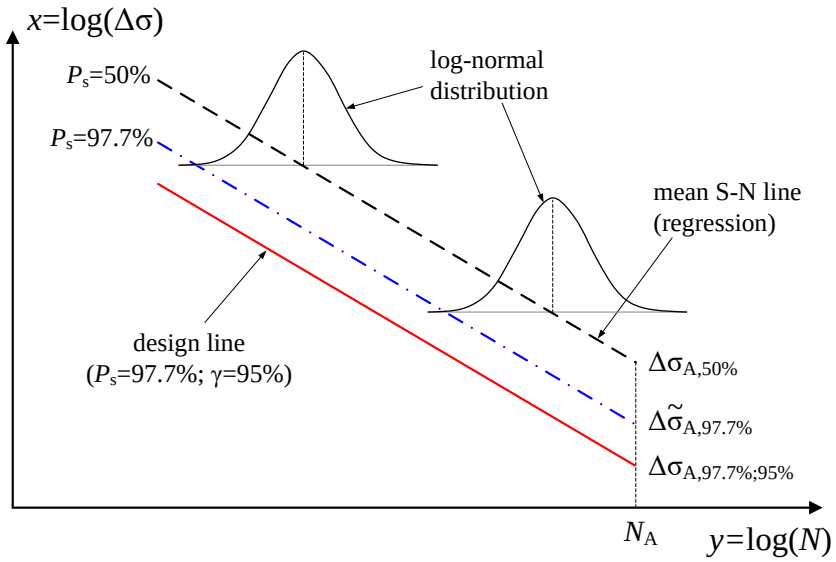

Figure 11: Mean S-N curve from the regression analysis and the design S-N curve at the prescribed probability P_s of survival (97.7%) and confidence γ (95%)

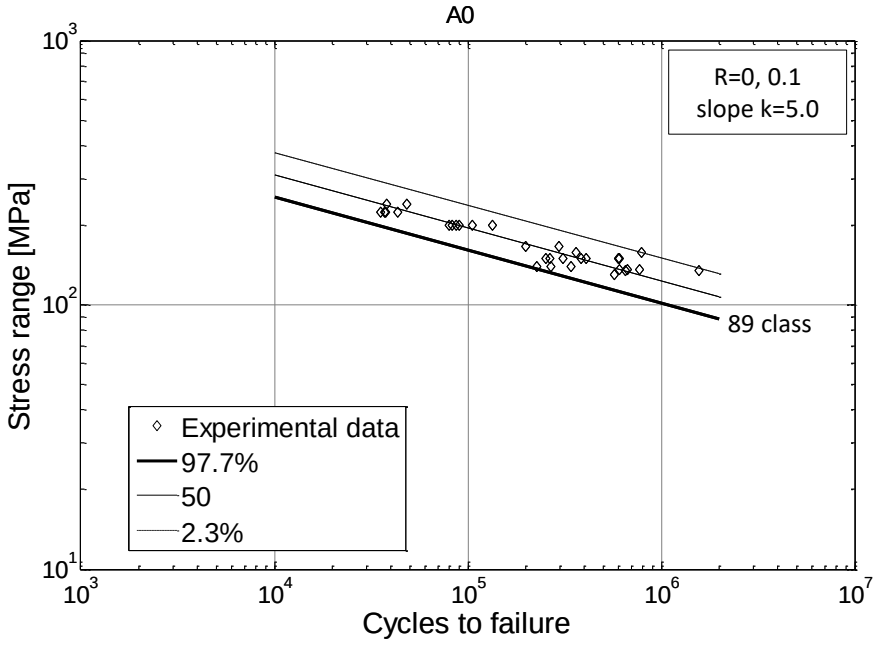

(a)

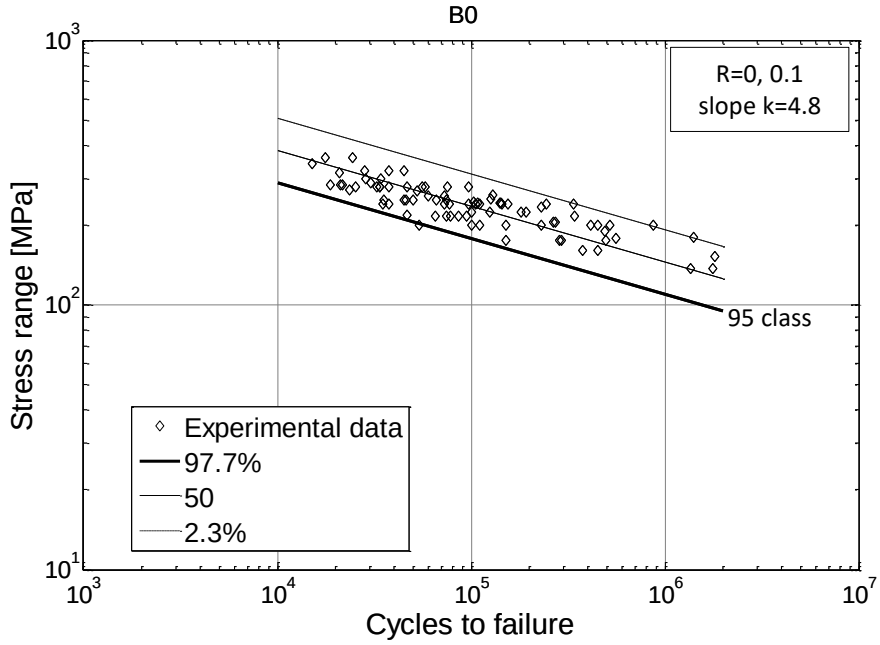

(b)

Figure 12: Fatigue curves for FS welds: (a) 5xxx series (category A0); (b) 2xxx and 6xxx series alloys naturally aged (category B0).

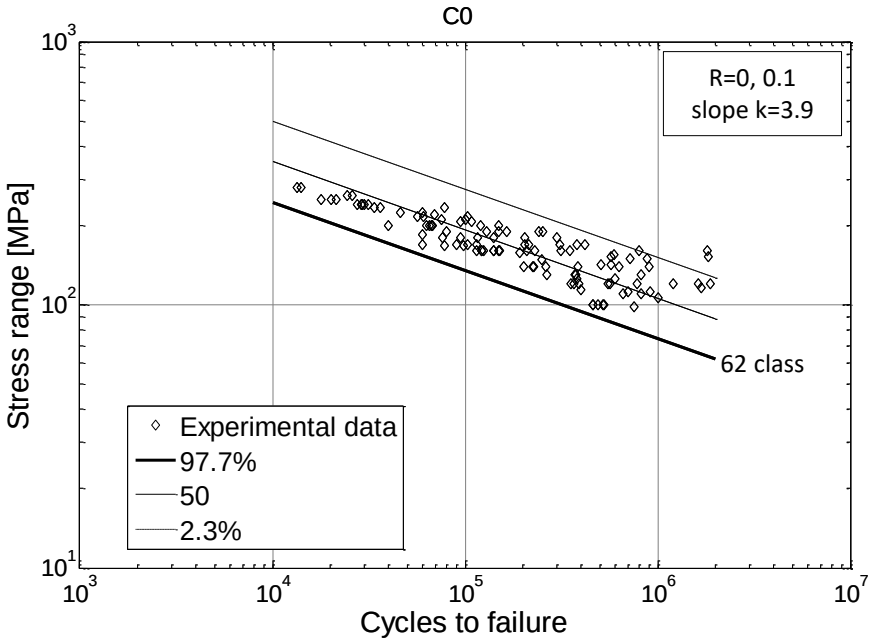

(a)

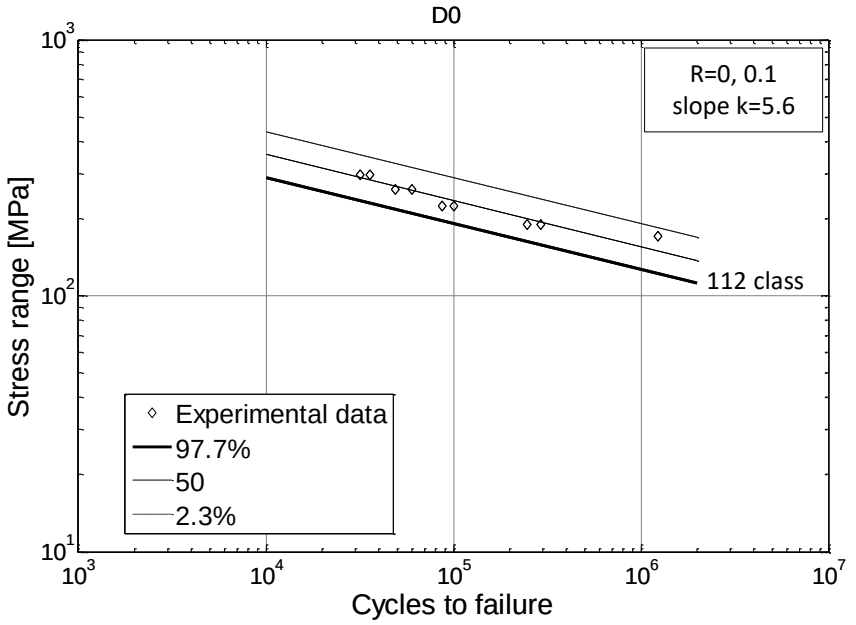

(b)

Figure 13: Fatigue curves for FS welds: (a) 2xxx and 6xxx series alloys artificially aged (category C0); (b) 7xxx series (category D0).

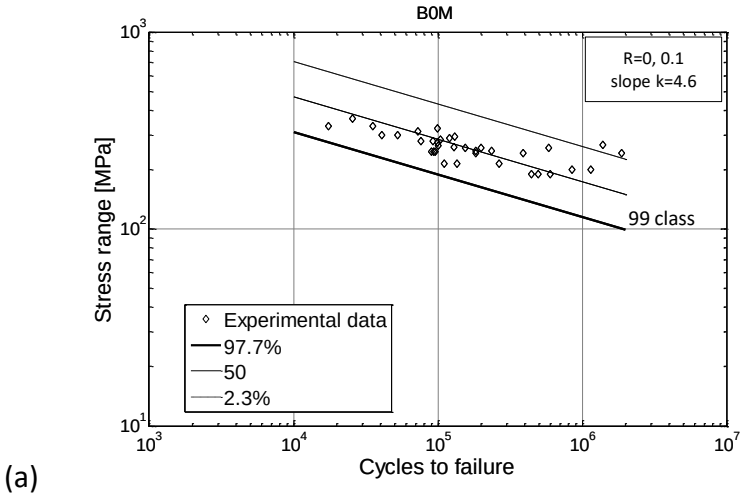

(a)

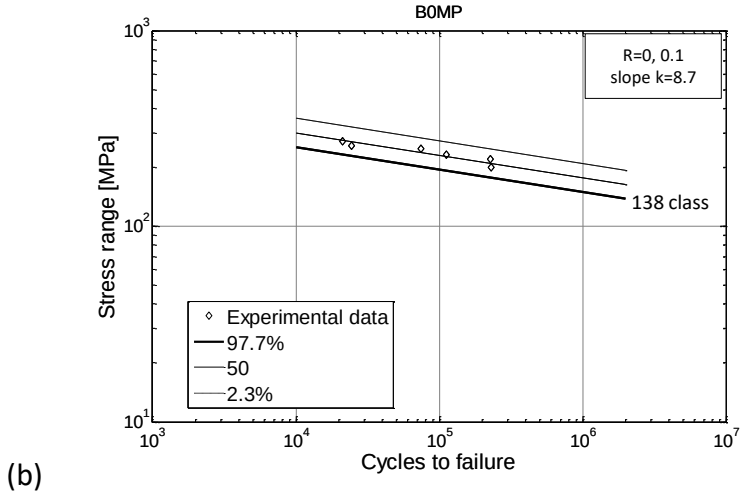

(b)

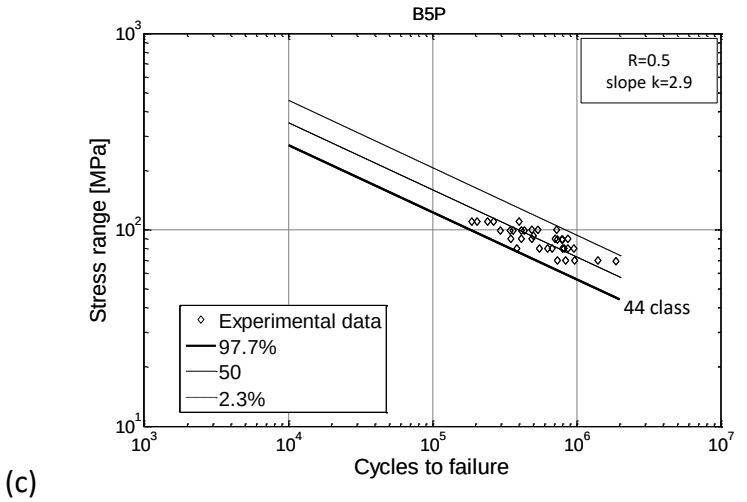

(c)

Figure 14: Fatigue curves for FS welds in 2xxx and 6xxx alloys (naturally aged): (a) machined welds (category B0M); (b) machined and post-weld treatment (category B0MP); (c) post-weld treatment (category B5P).

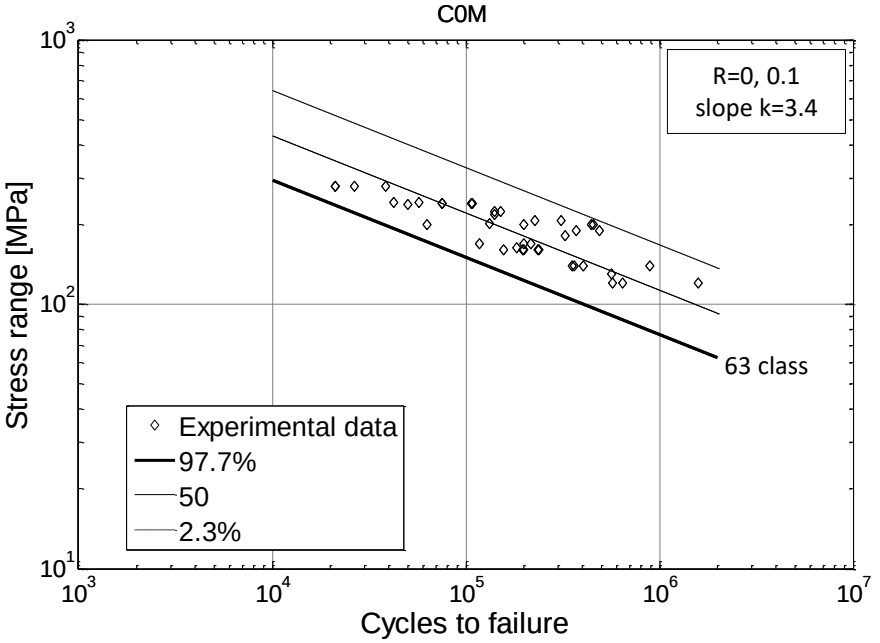

(a)

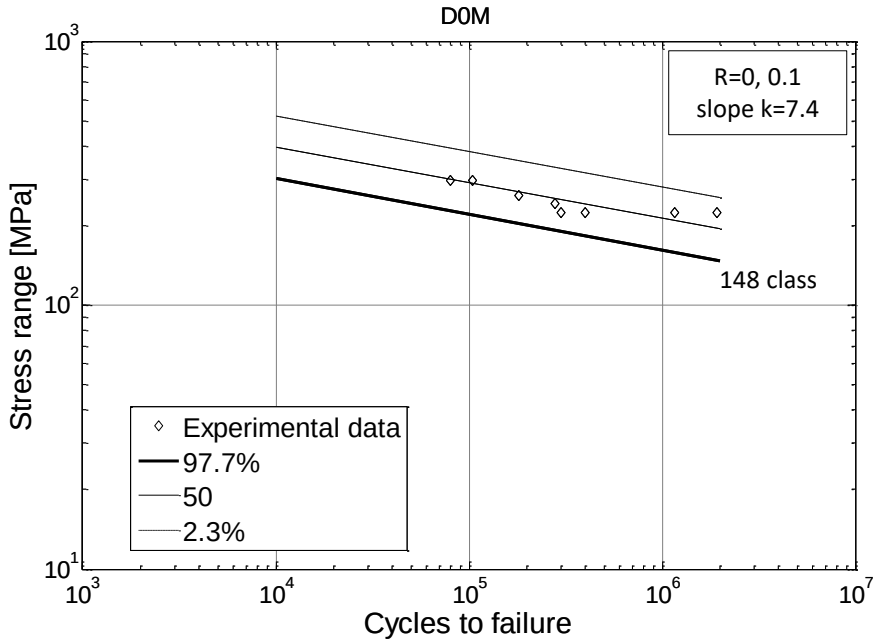

(b)

Figure 15: Fatigue curves for FS welds: categories: (a) 2xxx and 6xxx series alloys naturally aged, machined weld (category C0); (b) 7xxx series, machined weld (category D0M).

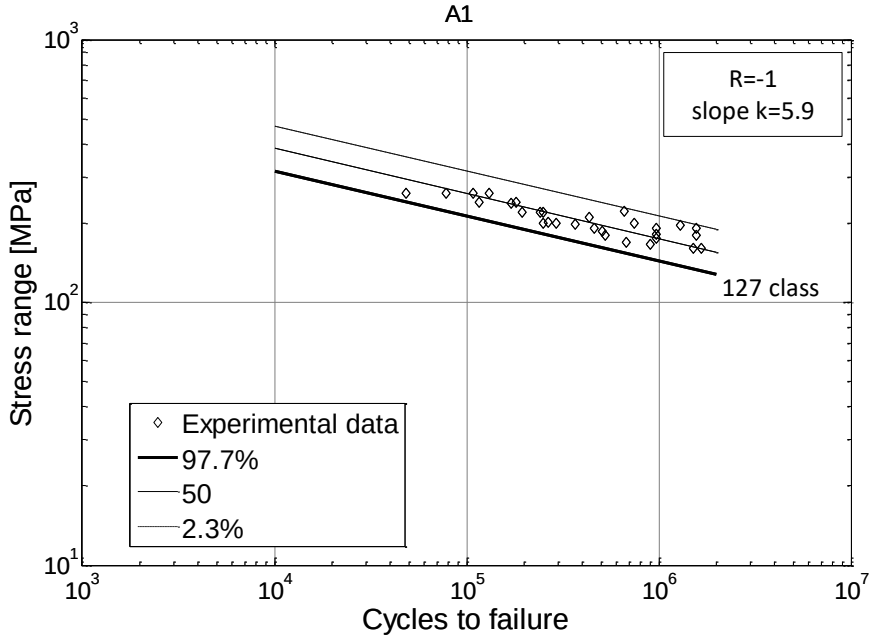

(a)

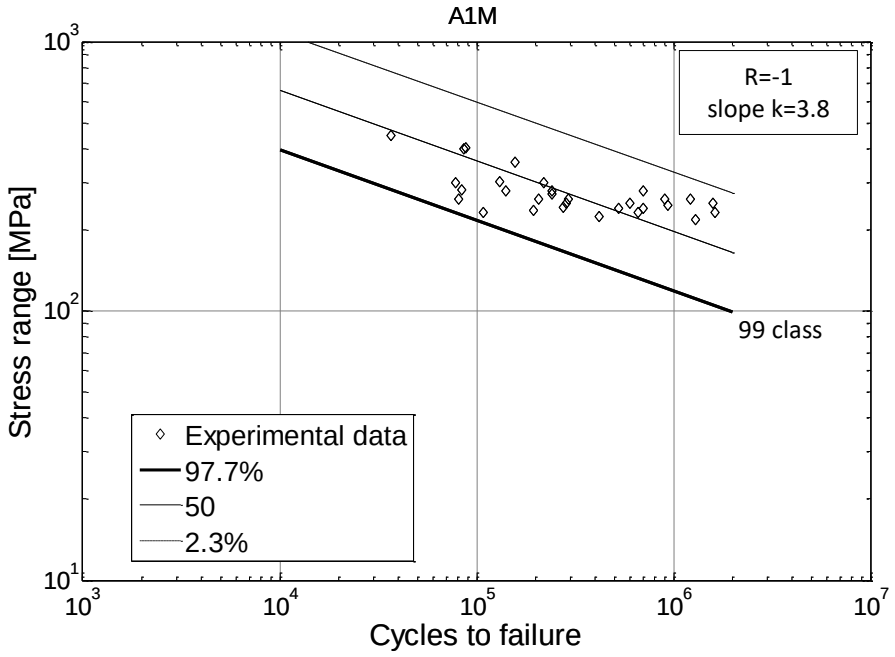

(b)

Figure 16: Fatigue curves for FS welds in 5xxx series alloys, tested at R=-1: (a) as welded (category A1); (b) machined (category A1M).

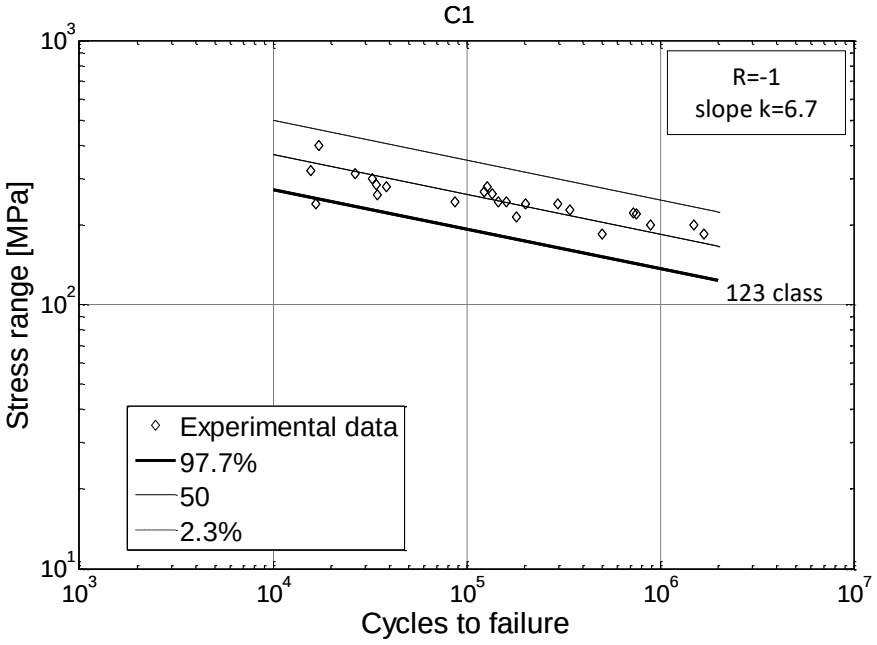

(a)

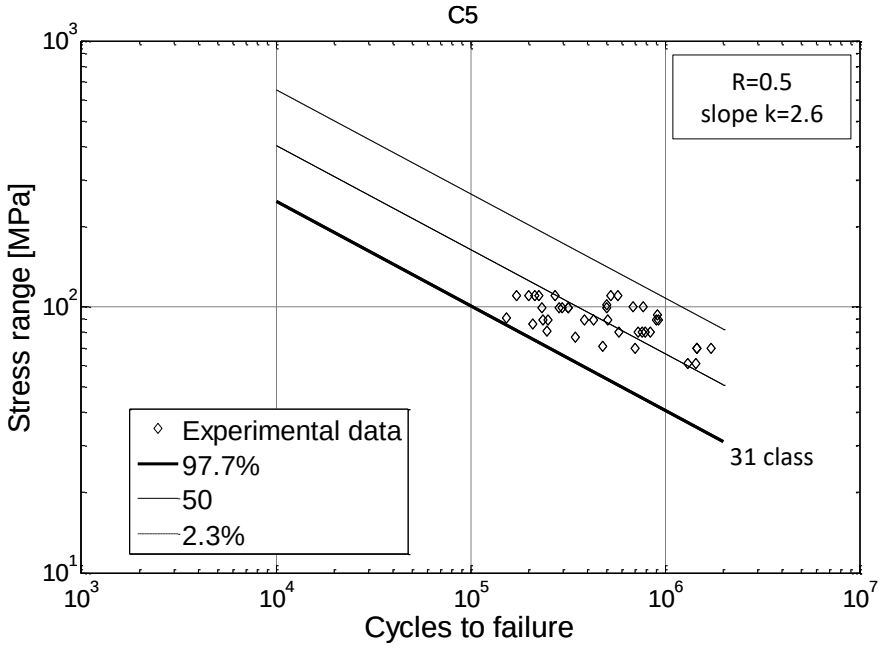

(b)

Figure 17: Fatigue curves for FS welds in 2xxx and 6xxx series alloys, artificially aged: (a) tested at R=-1 (category C1); (b) tested at *R* = 0.5 (category C5).

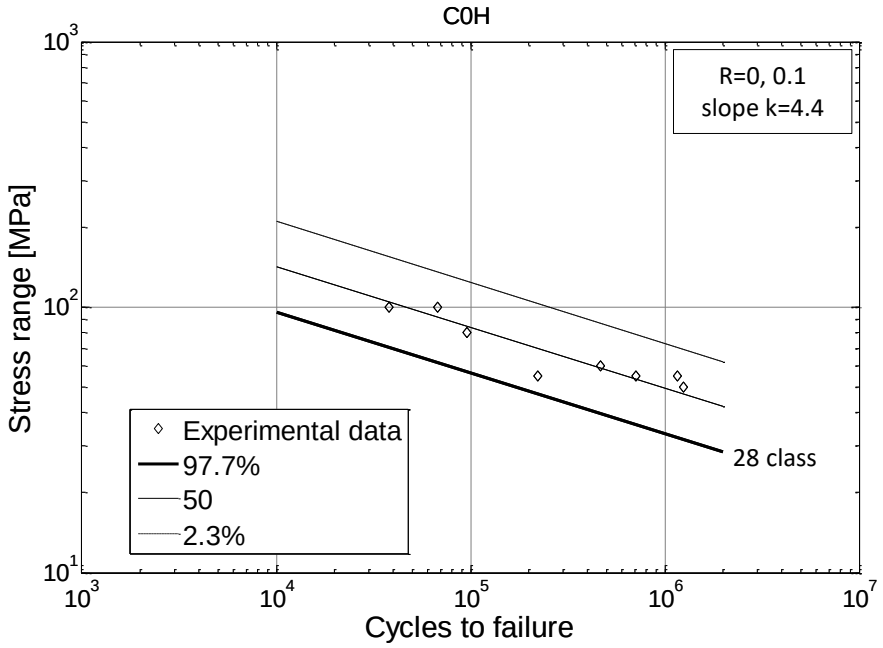

(a)

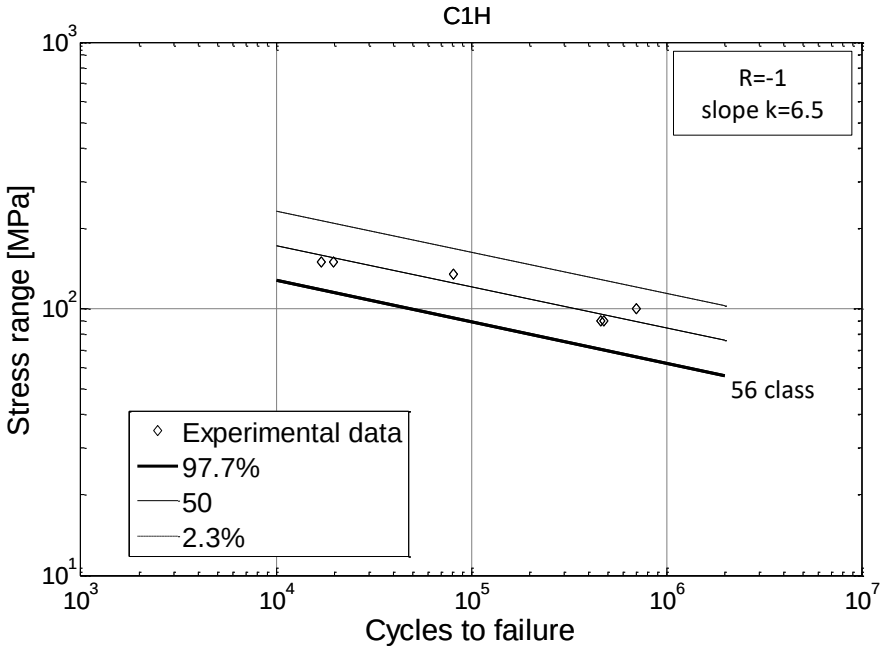

(b)

Figure 18: Fatigue curves for high curvature FS welds in 6xxx series, artificially aged: (a) tested at R = 0.1 (category C0H); (b) tested at R = -1 (category C1H).

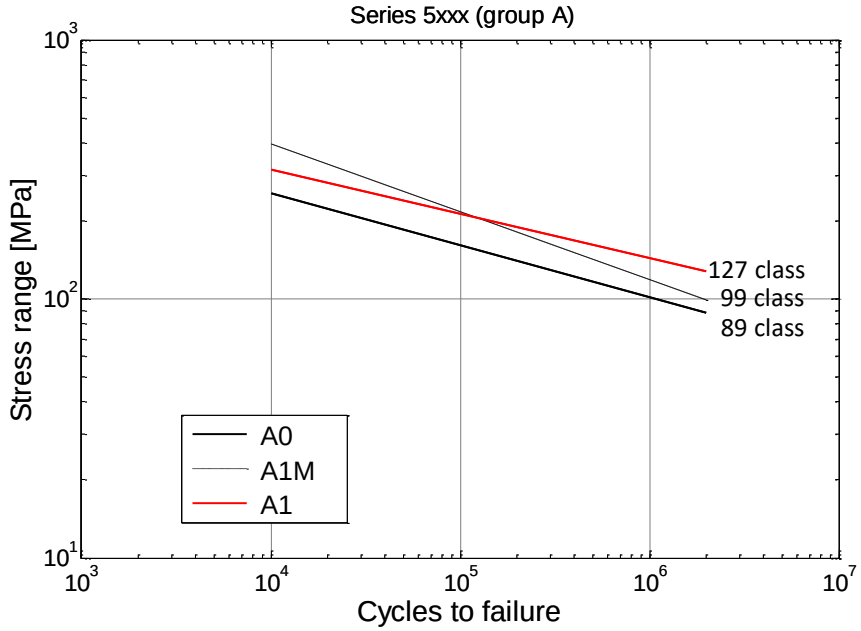
Series 5xxx (group A)
Stress range [MPa]
Cycles to failure
127 class
99 class
89 class
A0
A1M
A1

(a)

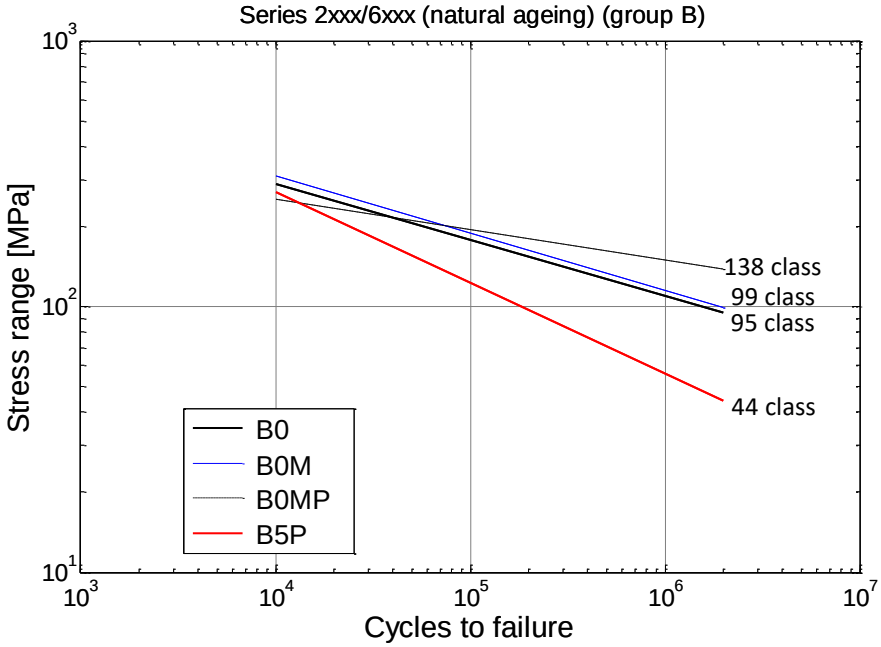
Series 2xxx/6xxx (natural ageing) (group B)
Stress range [MPa]
Cycles to failure
138 class
99 class
95 class
44 class
B0
B0M
B0MP
B5P

(b)

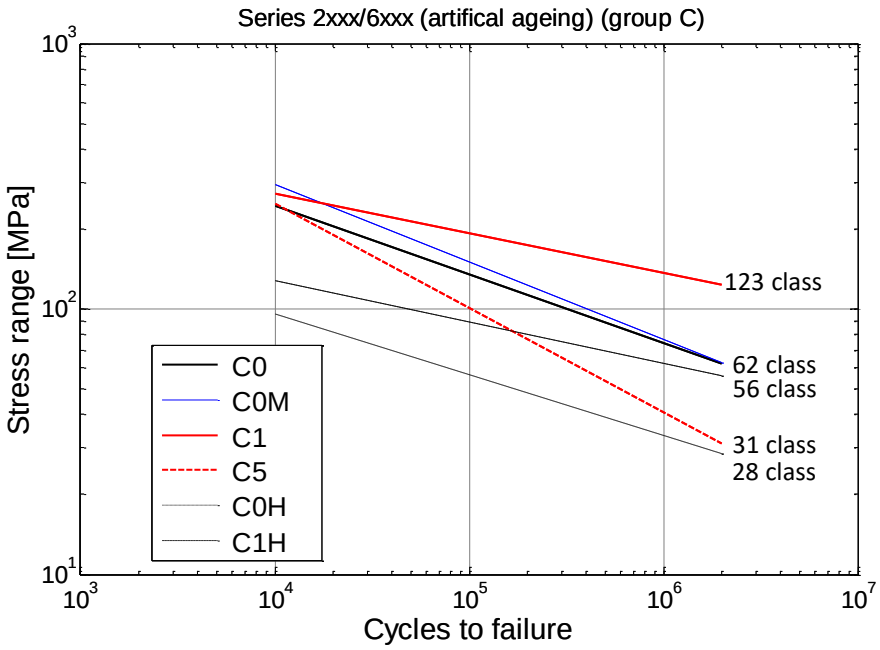

(c)

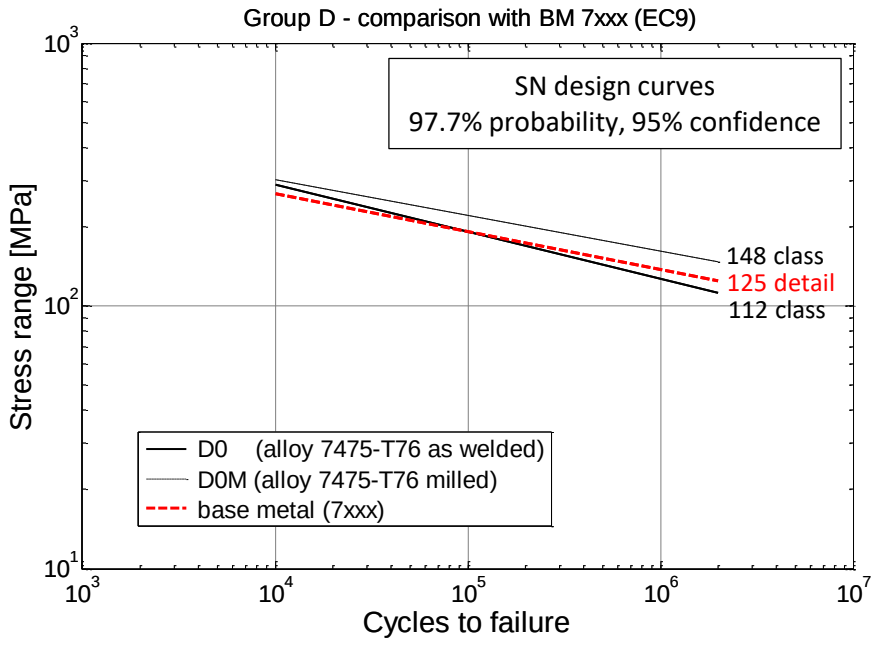

(d)

Figure 19: Comparison of fatigue curves (survival probability P_s=97.7%, confidence 95%) for each category A, B, C and D (for category D, the EC9 S-N design curves are also shown).

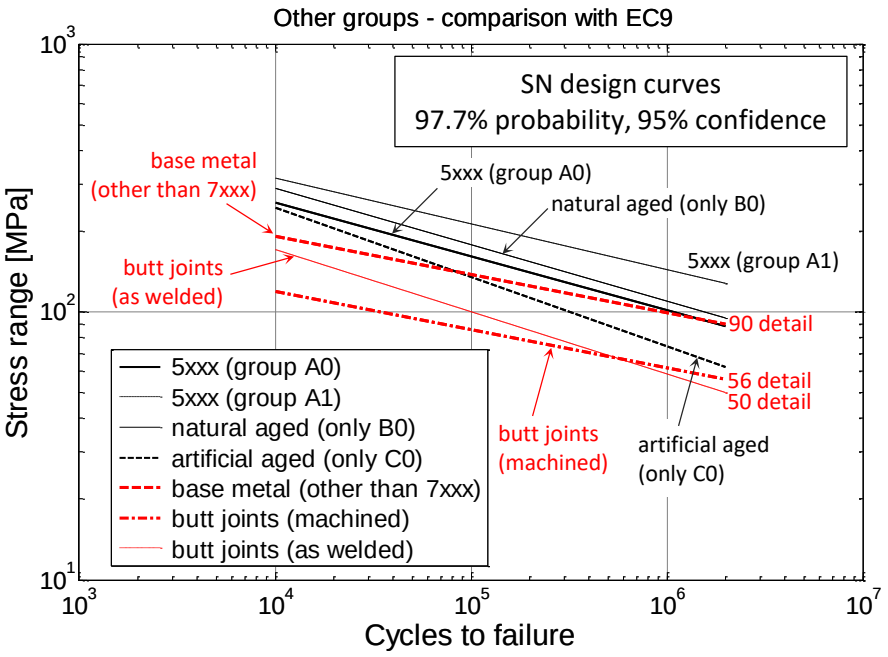
Other groups - comparison with EC9
SN design curves
97.7% probability, 95% confidence
base metal
(other than 7xxx)
5xxx (group A0)
natural aged (only B0)
5xxx (group A1)
butt joints
(as welded)
90 detail
56 detail
50 detail
butt joints
(machined)
artificial aged
(only C0)
5xxx (group A0)
5xxx (group A1)
natural aged (only B0)
artificial aged (only C0)
base metal (other than 7xxx)
butt joints (machined)
butt joints (as welded)
Stress range [MPa]
Cycles to failure

(a)

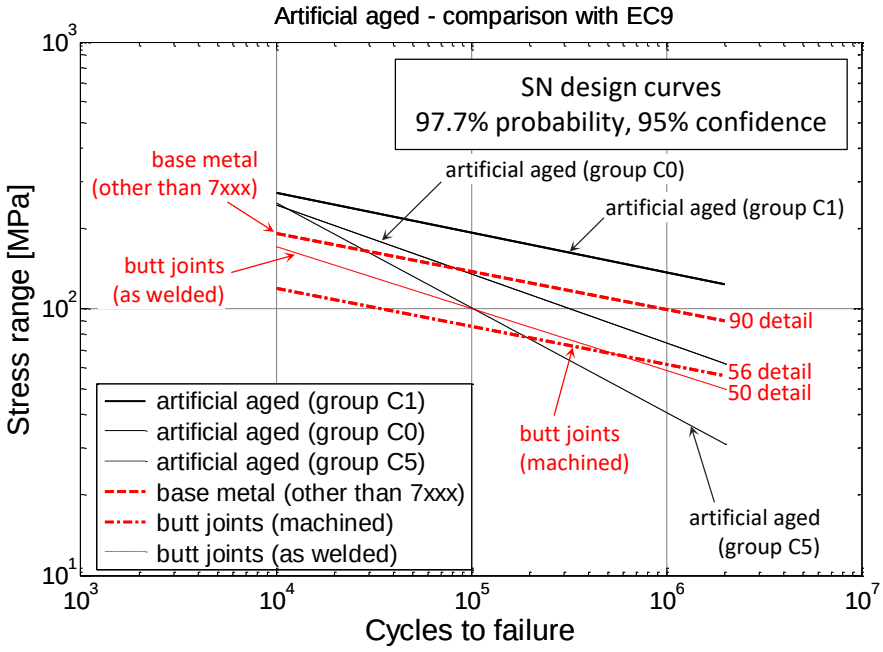
Artificial aged - comparison with EC9
SN design curves
97.7% probability, 95% confidence
base metal
(other than 7xxx)
artificial aged (group C0)
artificial aged (group C1)
butt joints
(as welded)
90 detail
56 detail
50 detail
butt joints
(machined)
artificial aged
(group C5)
artificial aged (group C1)
artificial aged (group C0)
artificial aged (group C5)
base metal (other than 7xxx)
butt joints (machined)
butt joints (as welded)
Stress range [MPa]
Cycles to failure

(b)

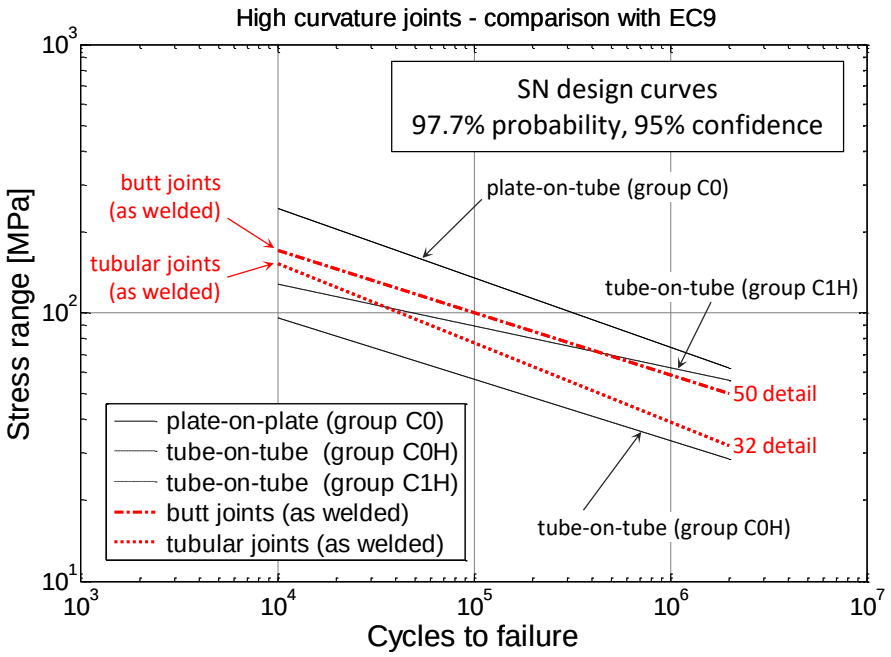

(c)

Figure 20: Comparison of the fatigue design S-N curves for fusion welds (extracted from EC9) and for friction stir welds (with survival probability P_s=97.7% and lower confidence 95%) for series 5xxx, and 2xxx and 6xxx series alloys in the natural or artificial aged conditions, and for tube-on-tube high curvature joints.